European Commission

Horizon 2020
European Union funding
for Research & Innovation

REDUCTION OF RADIOLOGICAL ACCIDENT CONSEQUENCES

Action	Research and Innovation Action NFRP-2018-1
Grant Agreement #	847656
Project name	**R**eduction of **R**adiological **C**onsequences of design basis and design extension **A**ccidents
Project Acronym	R2CA
Project start date	01.09.2019
Deliverable #	D3.6
Title	**Fuel rod behaviour during LOCA transient – Final report**
Author(s)	Arndt Schubert (JRC), François Kremer (IRSN), Andrius Tidikas (LEI), Davide Pizzocri, Giovanni Zullo (POLIMI), Jan Klouzal (UJV), Iurii Ovdiienko (SSTC), Francisco Feria (CIEMAT), Paul Van Uffelen (JRC)
Version	01
Related WP	WP3 LOCA
Related Task	T3.3. Fuel rod behaviour during LOCA transient (JRC)
Lead organization	JRC
Submission date	12.12.2022
Dissemination level	CO

This project has received funding from the Euratom research and training programme 2014-2018 under the grant agreement n° 847656

History

Date	Submitted by	Reviewed by	Version (Notes)
12.12.2022	A. Schubert (JRC)	S. Belon (IRSN)	01

Abbreviations

DBA	Design Basis Accident
DEC-A	Design Extension Accident
FG	Fission Gas
HBS	High Burnup Structure
IFPE	International Fuel Performance Experiments
LOCA	Loss Of Coolant Accident
PWR	Pressurized Water Reactor
PCMI	Pellet Clad Mechanical Interaction
RIA	Reactivity Initiated Accident
V&V	Verification & Validation
WWER	Water-cooled, Water-moderated Energy Reactor (Soviet designed PWR)
WP	Work Package

1. Introduction

The main objective of task 3.3 was to extend the knowledge and ability of simulation codes to predict the complex fuel behaviour during a LOCA transient. Among other items, it concerns:

- The fission gas release causing additional cladding internal loading,
- The quantity and nature of radionuclide released within LOCA conditions (including rapid transients, high temperature and HBS),
- The impact of fuel fragmentation on oxidation, fission gas and solid fuel fragment releases.

To this end, fuel performance codes have been extended to include a higher degree of mechanistic modeling. In the course of the R2CA project, the following steps have been taken and are addressed in this report:

- Re-assessing an appropriate experimental database that includes completed simulation exercises (Section 2)
- Extending mesoscale and mechanistic fuel behavior codes (MFPR-F and SCIANTIX, respectively) to improve their coverage of LOCA conditions (Sections 3.1 and 3.2)
- Extending the mechanical modelling in an integral fuel performance code (FRAPTRAN, Section 3.3)
- Developing a prototype standalone module for axial gas communication during LOCA (Section 3.4)
- Developing plug-in modules for coupling mechanistic and mesoscale codes to integral fuel performance codes (TRANSURANUS and FRAPTRAN, Section 4)
- Verification and validation of the coupled code versions, including first uncertainty and sensitivity analyses for the LOCA phase (Section 5)
- Developing service modules for off-line interfaces used by the TRANSURANUS code (Section 6)

Six organizations were involved in this task (JRC, IRSN, POLIMI, UJV, CIEMAT, SSTC and LEI).

2. Re-assessment of an experimental database

The following simulation cases have been identified as appropriate for V&V of the first phase of developments regarding fuel behavior during LOCA. Three cases stem from the IAEA coordinated research project (CRP) on fuel rod modelling in accident conditions (FUMAC) with details given in the final project report [1]:

a) Two experiments of the Halden Reactor test series IFA-650 (part of the joint international programme) of the Halden Reactor Project. Both addressed the LOCA performance of high burnup fuel irradiated in commercial nuclear power and were part of the IAEA CRP FUMAC.
   - IFA-650.10 (PWR fuel segment pre-irradiated to 61 MWd/kgU) indicating moderate ballooning, fuel fragmentation and dispersal
   - IFA-650.11 (WWER fuel segment pre-irradiated to 56 MWd/kgU): indicating little ballooning and fuel fragmentation

b) One LOCA simulation test (NRC-192) performed by Studsvik Nuclear AB, Sweden, under contract with the U.S. Nuclear Regulatory Commission (NRC). The element used in test #192 was sampled from the middle section of a full-length Westinghouse 17x17 PWR UO_2 fuel rod with the first generation ZIRLO cladding, which had been operated to a rod average discharge burnup of 68.2 MWd/kgU during four reactor cycles at a twin-unit plant in the USA.

Moreover, two groups of irradiation experiments performed at the French Siloe reactor were identified from the NEA International Fuel Performance Experiments (IFPE) Database [2]:

a) HATAC C1 and C2 experimental rods with two fuel segments taken from pre-irradiated 17x17 PWR fuel rods to measure the magnitude and kinetics for the release of both stable and radioactive fission gas during a succession of short transients (high burnup power cycling).
b) Contact 1, as part of the cooperative project of CEA and Framatome concerning the understanding of the performance of 17x17 fuel assembly behaviour in PWR constant irradiation conditions [3]. The tests involved an in-pile study of the behaviour of short fuel rods with five UO_2 pellets with a Zr4 cladding.

3. Model and code developments

3.1 Extensions for the mesoscale code MFPR-F (IRSN)

The MFPR-F code of IRSN is derived from the MFPR code developed by M. Veshchunov and coworkers [4]. At present, it is used as a point model in TRANSURANUS (via direct coupling), calculating the fission product and crystal defects behaviours at the grain scale, in each segment of the TRANSURANUS meshing.

As an extension to such usage, further developments have been performed in the coupling, enabling the use of MFPR-F models defined at the pellet scale, in particular the model for radial redistribution of oxygen, which is of primary interest for the modelling of fuel oxidation and its effect on conductivity and FP behaviour. Such developments also enabled the activation of MFPR-F models related to HBS zone [5], namely its formation under irradiation and the FG behavior during thermal transient, which are of primary interest for the study of LOCA events, as it has been highlighted in the 2021 progress report of the current task. On the practical side, the pellet scale models of MFPR-F require a specific radial discretization of a pellet. In the context of the coupling, interpolation of data between the TRANSURANUS and MPFR-F meshes is thus needed, as illustrated on the figure below, on which both coupling modes, point and slice, are represented, along with the involved data transfers.

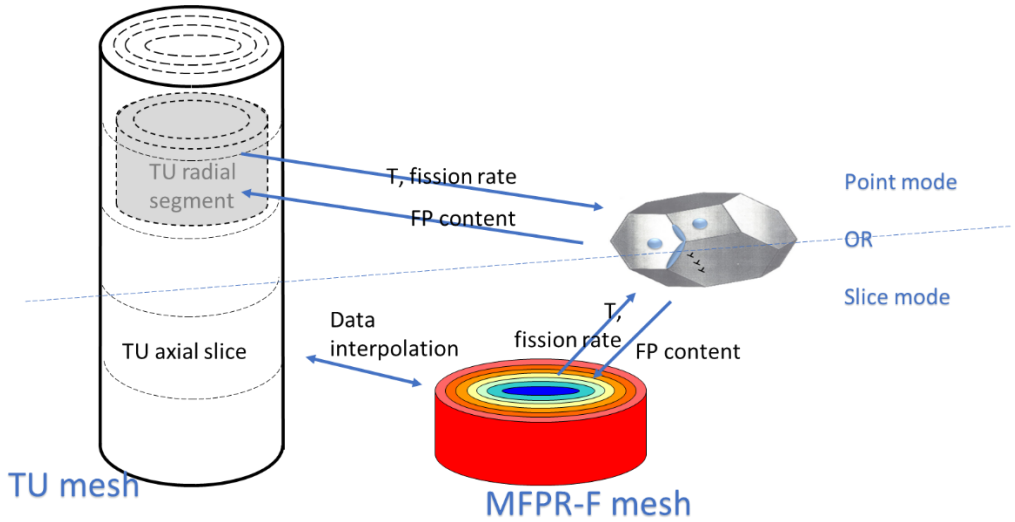

Figure 1. Scheme for the TRANSURANUS//MFPR-F coupling in point mode (top) or slice mode (bottom).

3.2 Extensions for the mesoscale code SCIANTIX (POLIMI)

Fission gas behaviour modelling activities at POLIMI are focused on the development of the SCIANTIX code [6] and also on its coupling with TRANSURANUS. In detail, the compatibility of the restart capability in TRANSURANUS//SCIANTIX has been addressed during the R2CA project. The restart option is needed for simulation of irradiation experiments where a fuel rod has been refabricated or the filling gas completely changed. Illustrative cases include the IFA-650.10/11 [1] and the HATAC C2. Moreover, extending the available validation database has been key to assess new models for the mechanistic behavior of radioactive fission gases [7,8] and fosters testing of models for formation and evolution of the high-burnup structure related to PCMI and fuel fragmentation under LOCA conditions.

The SCIANTIX code is a mesoscale open-source code for the mechanistic description of the fission gas behaviour within the fuel grain. It has been developed at POLIMI. Since the standalone development of the first version of the SCIANTIX code, a specific API has also been developed for the coupling with different fuel performance codes such as TRANSURANUS and GERMINAL.
SCIANTIX is based in C++ whereas TRANSURANUS in modern Fortran. The interface for the code coupling relies on the BIND(C) attribute and on the ISO_C_BINDING module of modern Fortran. The BIND(C) attribute enables C calling conventions and changes symbol names. The ISO_C_BINDING module provides access to named constants representing type parameters of data representations compatible with C types, thereby smoothing the interoperability between the two languages.
To minimize the effect on the existing structure of the TRANSURANUS code, and in line with the strategy adopted for the coupling with MFPR-F outlined above, it was decided to implement a new set of global variables pertaining to the quantities calculated by the SCIANTIX code. These global variables are then – if needed – casted back into the existing variables of the TRANSURANUS code. To this end, the Fortran module CommonData_FP3 has been introduced as an additional “global variables” module.
The driver routine for the calls to the SCIANTIX calculations in TRANSURANUS is contained in the new subroutine, named FisPro3.f95.
Two new routines have been created to transfer arrays of variables from one code to the other, considering also the unit conversion. On the one hand, the arrays of variables to be passed to the SCIANTIX code from the TRANSURANUS code are handled by the new SetSciantixVariablesfromTU routine. The variables contain the values at the previous time step of the state variables, the input settings, and the irradiation history conditions (local temperature, fission rate density, hydrostatic stress, local burnup, and time step), and are filled with the variables declared in the CommonData_FP3 and GlobalData modules in the (new) SetSciantixVariablesfromTU routine. On the other hand, the relevant GlobalVariables and CommonData_FP3 variables are updated after the SCIANTIX calculations in the SetTUVariablesfromSCIANTIX routine.

To ensure the compatibility of the restart option between TRANSURANUS and SCIANTIX, the TRANSURANUS arrays containing SCIANTIX informations have been extended i.e., r8_comp and r4vek. The array r8_comp includes the SCIANTIX variables, which are declared in TRANSURANUS as double precision data. These variables are stored in 100% densely packed form in memory (within the r8_comp array) during the analysis of each axial slice (or section) by the subroutines datput.f95, datpix.f95, datpre.f95 and datpwr.f95, which drive the compressing and unfolding procedure. Eventually, the rstart.f95 subroutine reads / writes variables in case of restart and, by accessing the r8_comp and r4vek arrays, transfers the information between the instant of restart (t_{intrup}).

Summarizing, adding the restart option in TRANSURANUS coupled with SCIANTIX required the definition of new variables and several routine modifications, performed in collaboration with JRC and presented at the international workshop “Towards nuclear fuel modelling in the various reactor types across Europe”, 28-30 June 2021.

3.3 Extensions for the fuel performance code FRAPTRAN (CIEMAT)

3.3.1 Original mechanical modelling

3.3.1.1 Introduction

The FRAPTRAN code is a transient fuel performance predictive tool developed by PNNL to be applied to design basis accident conditions (RIA, LOCA) [9]. It uses the FRACAS-I model to predict the mechanical response of fuel and cladding for small strains and the BALON2 model to predict clad ballooning (i.e., large strains). Both models are fed with MATPRO´s correlations for Zircaloy cladding [10].

Figure 2 depicts how the mechanical modelling of FRAPTRAN works. As it is shown, at the end of each load increment calculation, cladding effective plastic strain, ε^p, is obtained by FRACAS-I and compared to the instability strain, ε^p_{inst} (set to 5%). If the calculated strain does not reach the instability strain, cladding deforms accordingly and a new load is calculated by FRACAS-I model. However, if the calculated strain is greater than this limit, it is assumed that ballooning occurs (large localized non-uniform deformation) at that axial node. Then, BALON2 model is used; FRACAS-I is no longer used for cladding (the corresponding calculations stop for all the nodes) and BALON2 performs strain calculations only for the ballooning node. BALON2 predicts clad failure when either cladding true hoop stress or cladding plastic hoop strain are over respective empirical thresholds (Figure 3).

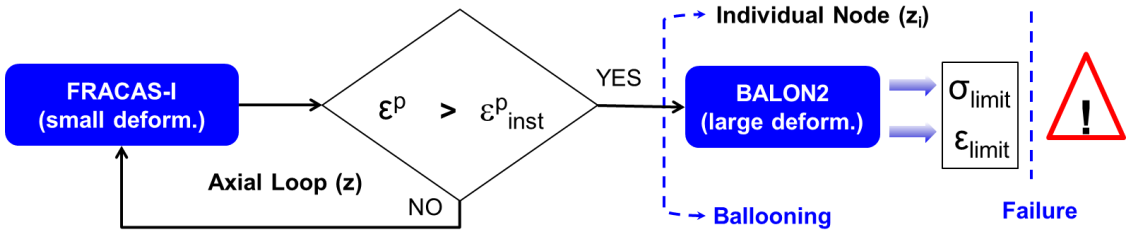

Figure 2. Scheme for the FRATRAN´s mechanical modelling.

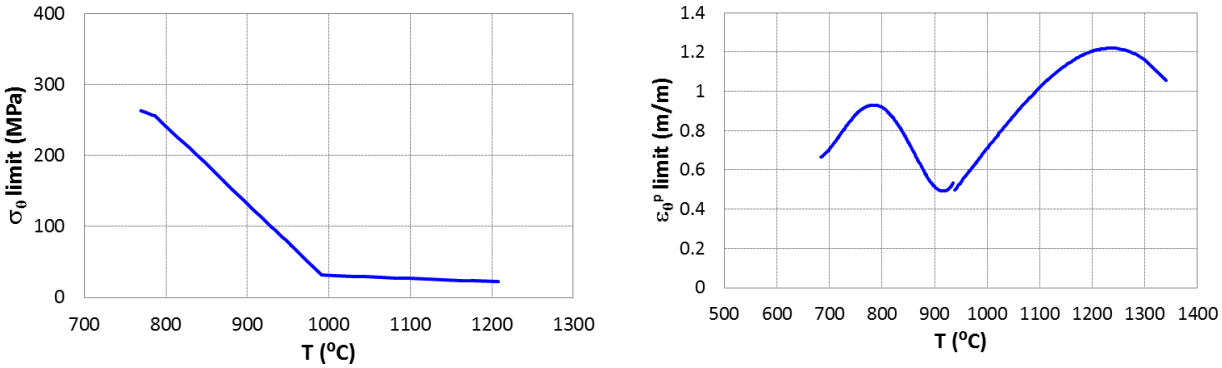

Figure 3. BALON2 empirical limits: true hoop stress limit (left) and plastic hoop strain limit (right).

The following sections show the details of the mechanical modelling of FRAPTRAN according to the models cited above with the focus on the cladding plastic deformation up to failure, as one of the main targets under LOCA conditions.

3.3.1.2 FRACAS-I model

The cladding deformation model in FRACAS-I is based on the incremental theory of plasticity, applied in each axial node (neither circumferential nor radial nodalization of the cladding is considered in the modelling according to the axisymmetry approach and the thin-shell theory, respectively). The relationship between the components of the plastic strain increments, $d\varepsilon^p_i$ (i: hoop, θ, axial, z, radial, r), and the effective plastic strain increment, $d\varepsilon^p$, is provided by the Prandtl-Reuss isotropic flow rule:

$$d\varepsilon_i^p = \frac{3}{2}\frac{d\varepsilon^p}{\sigma_{eff}}\left[\sigma_i - \frac{1}{3}\left(\sigma_\theta + \sigma_z + \sigma_r\right)\right] \quad (1)$$

where σ_i are the cladding stress components and σ_{eff} is the effective stress. Additionally, the condition of incompressibility is fulfilled:

$$d\varepsilon_\theta^p + d\varepsilon_z^p + d\varepsilon_r^p = 0 \quad (2)$$

The cladding stress components are calculated based on the pressure difference between the fuel side (rod internal pressure, P_i, assuming no pellet-clad mechanical contact under LOCA conditions) and the water side (external pressure, P_o):

$$\sigma_\theta = \frac{r_i P_i - r_o P_o}{r_o - r_i}$$
$$\sigma_z = \frac{r_i^2 P_i - r_o^2 P_o}{r_o^2 - r_i^2} \quad (3)$$

with r_i and r_o the uniform inner and outer cladding radius, respectively. Note that the radial stress, σ_r, is assumed to be negligible according to the approach carried out by the code (i.e., shell theory). Based on the stress components, the cladding effective stress is calculated as:

$$\sigma_{eff} = \sqrt{\frac{\left(\sigma_\theta - \sigma_z\right)^2 + \left(\sigma_z - \sigma_r\right)^2 + \left(\sigma_r - \sigma_\theta\right)^2}{2}} \quad (4)$$

The effective plastic strain increment is determined from the basic MATPRO´s equation that relates stress and plastic strain:

$$\sigma_{eff} = K \cdot \left(\varepsilon^p\right)^n \cdot \dot{\varepsilon}^m \quad (5)$$

where K is the strength coefficient, n the strain hardening exponent and m the strain rate exponent, being $\dot{\varepsilon}$ the strain rate. These coefficients depend on temperature, fast neutron fluence and material cold work as well as an eventual phase transition. The last two are encompassed to account for the corresponding hardening effect, although both variables are also correlated with the temperature to simulate the hardening recovery under high temperature conditions (annealing). The details of these parameters are reported elsewhere [10,11]. By default, during the open-gap regime, the plastic strain increment in FRACAS-I is not computed according to this equation (see section 3.3.1.3).

It should be noted that the FRACAS-I model implemented in FRAPTRAN does not take into account the viscoplastic strain, that is to say, creep is not modelled.

3.3.1.3 BALON2 model

As previously mentioned, the BALON2 model calculates the non-uniform large cladding deformation that occurs between the time that the cladding plastic strain exceeds the instability strain and the time of cladding rupture, if it is eventually predicted. The model divides the ballooning axial node into circumferential nodes and axial sub-nodes, as shown in Figure 4. The cladding is assumed to consist of a network of "membrane elements" subjected to a pressure difference between the inside surface and the outside surface.

The plastic strain increment components are determined by the Prandtl-Reuss flow rule taking into account the anisotropies of the cladding material according to MATPRO´s formulation [10]:

$$d\varepsilon_\theta^p = \frac{d\varepsilon^p \cdot \left[a\cdot(\sigma_\theta - \sigma_z) + b\cdot(\sigma_\theta - \sigma_r)\right]}{\sigma_{eff}}$$
$$d\varepsilon_z^p = \frac{d\varepsilon^p \cdot \left[c\cdot(\sigma_z - \sigma_r) + a\cdot(\sigma_z - \sigma_\theta)\right]}{\sigma_{eff}} \quad (6)$$
$$d\varepsilon_r^p = \frac{d\varepsilon^p \cdot \left[b\cdot(\sigma_r - \sigma_\theta) + c\cdot(\sigma_r - \sigma_z)\right]}{\sigma_{eff}}$$

with a, b and c anisotropy coefficients. The condition of incompressibility is not applied in this model. The stress and strain are calculated with the basis shown in the previous section but taking into account the non-uniform shape of the cladding at ballooning [12]. Particularly, radial and hoop stress are estimated as follows:

$$\sigma_r = -\frac{r_i' P_i + r_o' P_o}{r_o' + r_i'} \quad (7)$$

$$\sigma_\theta = \frac{r_i' P_i - r_o' P_o}{r_o' - r_i'} - \frac{(P_i - P_o)(\delta - (r_o' - r_i'))\cdot r_{av}}{(r_o' - r_i')^2} + \frac{r_{av}\cdot\sigma_z}{[\exp(\varepsilon_z)]^2}\frac{\partial^2 r_{av}}{\partial z^2} \quad (8)$$

with r_i' and r_o' the non-uniform inner and outer cladding radius, δ the local thickness (non-uniform due to the ballooning shape), r_{av} the midwall radius and ε_z the total axial strain.

In order to obtain the effective plastic strain increment according to the mechanical behavior anticipated in the ballooning zone, i.e., the high-temperature creep strain, the BALON2 model uses the following equation from MATPRO [10]:

$$d\varepsilon^p = \left[\left(\frac{n}{m}+1\right)10^{-3}\left(\frac{\sigma_{eff}}{K}\right)^{1/m} dt + \varepsilon_{i-1}^{\left(\frac{n}{m}+1\right)}\right]^{\frac{m}{m+n}} \quad (9)$$

This equation is based on the same concept as equation 5, using the coefficients K, n, and m, previously mentioned. In other words, the formulation used in BALON2 model to estimate viscoplasticity is based on parameters fitted to stress-strain curves. Note that FRAPTRAN has the option to use equation (9) instead of equation (5) in FRACAS-I; indeed, it is the option selected by default in the code during the open gap regime.

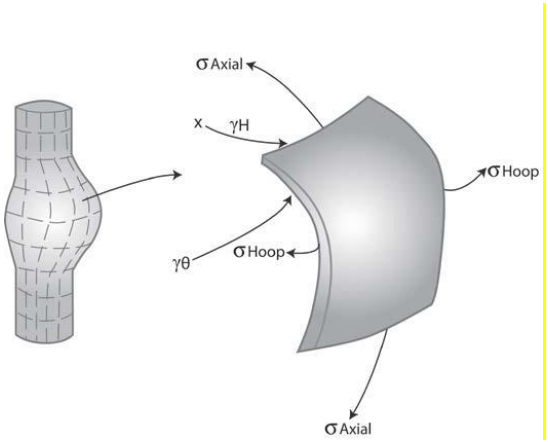

Figure 4. Scheme for the BALON2 nodalization.

According to the review carried out, the mechanical approach used in a fuel performance code like FRAPTRAN to predict the cladding mechanical performance under ballooning regime is consistent. However, when it comes to the formulation used to determine the cladding viscoplastic behavior, alternative modelling should be explored.

Aside hypotheses made, fundamentals of cladding mechanics are soundly supported generally speaking. However, when dealing with viscoplastic behavior, the implicit empirical approach intended might be enhanced.

3.3.2 Extensions for mechanical models of FRAPTRAN

In order to explore alternative creep modelling, the Norton´s law has been implemented in FRAPTRAN as an option. Additionally, the bias of both creep models (i.e., default and Norton) and the bias of the failure limits have also been implemented to check the corresponding uncertainty in the predictions made. The following sections show the details of the adaptations carried out.

3.3.2.1 Alternative creep law

One of the most commonly used creep models for Zircaloy cladding under LOCA conditions is the Norton´s creep law, applied in fuel performance codes like TRANSURANUS [13] or BISON [14]. Using the variables shown in the previous section, it is formulated as follows:

$$d\varepsilon^{p} = A \cdot \exp\left(-\frac{Q}{R \cdot T}\right) \cdot \sigma_{eff}{}^{n} \cdot dt \qquad (10)$$

where A, Q and n are coefficients that depend on temperature, strain rate and the α-β phase, which in turn depends on temperature and hydrogen content [14].

Figure 4 depicts the comparison between the Norton´s creep law and the MATPRO´s correlation (equation 9). As boundary conditions, a linear temperature rise from 300ºC to 1000ºC and a constant hoop stress of 50 MPa have been applied. The MATPRO´s correlation has also been fed with null fast neutron fluence and cold work, that is to say, an unirradiated RXA Zircaloy cladding has been considered; furthermore, an additional case with irradiated

RXA Zircaloy has been included with a fast neutron fluence of 10^{26} n/m^2. As it can be observed from Figure 5, there are huge differences between the estimations of the Norton´s creep law and the MATPRO´s correlation, both from a quantitatively and qualitatively point of view. The model from MATPRO predicts the highest deformation for unirradiated material, whereas for the irradiated cladding the prediction gives rise to lower deformation than the Norton creep´s law (irradiation hardening effect included in the MATPRO´s correlation).

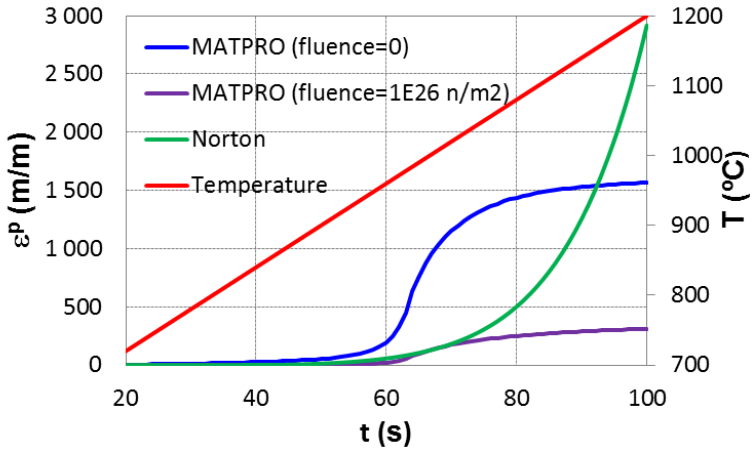

Figure 5. Creep models comparison.

3.3.2.2 Introduction of a bias

Bias in the creep model

The bias of the MATPRO´s creep model (equation 9) has been accounted for in this work through the information made available in [10]. Particularly, the following bias concerning K, n and m parameters (called UK, Un and Um, respectively) has been implemented in FRAPTRAN:

$$UK=\begin{cases}77\cdot10^{6}\ ,\ T<427\,ºC\\110.4\cdot10^{6}-4.8\cdot10^{4}\cdot T\ ,\ 427\le T\le 527\,ºC\\K/3\ ,\ T>527\,ºC\end{cases} \quad (11)$$

$$Un=\begin{cases}0.017,\ T<427\,ºC\\-2.8\cdot10^{-2}+6.5\cdot10^{-5}\cdot T\ ,\ 427\le T\le 982\,ºC\\0.053\ ,\ T>982\,ºC\end{cases} \quad (12)$$

$$Um=\begin{cases}0.01,\ T<427\,ºC\\-2.98\cdot10^{-2}+5.7\cdot10^{-5}\cdot T\ ,\ 427\le T\le 627\,ºC\\0.16\cdot m\ ,\ T>627\,ºC\end{cases} \quad (13)$$

It should be noted that the parameters K, n and m also affect the mechanical calculations in FRACAS-I, so the corresponding bias will also have an impact in the small deformations estimated by the code.

Regarding the bias of the Norton´s creep law (equation 10), it has been estimated based on creep data gathered from [15]. Figure 6 shows a non-negligible scattering of the model with respect to the data. Based on that, the standard deviation has been derived, from which the bias of the creep law has been expressed as follows:

$$\dot{\varepsilon}^{p+} = \dot{\varepsilon}^{p} \cdot (1 + cf \cdot rstd)$$
$$\dot{\varepsilon}^{p-} = \dot{\varepsilon}^{p} / (1 - cf \cdot rstd) \quad (14)$$

where $\dot{\varepsilon}^{p+}$ and $\dot{\varepsilon}^{p-}$ are the upper and lower bounds of the creep rate, respectively, rstd is the relative standard deviation (a value of 3.01 is estimated) and cf is the coverage factor. In Figure 6, the dashed lines represent the bias with a cf of 1 (68% of the scattering is covered).

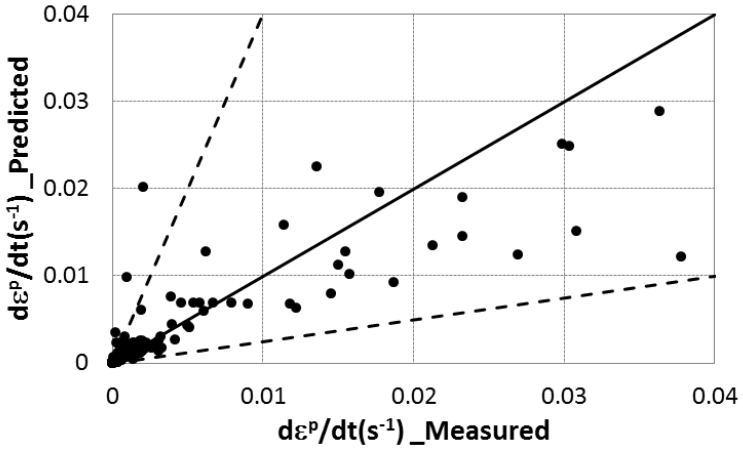

Figure 6. Model-to-data comparison of the Norton creep law.

Figure 7 represents the comparison between the MATPRO´s correlation and the Norton´s creep law, taking into account the bias of both. The boundary conditions applied are the same as in the previous section. It should be noted that the bias cannot explain the important differences previously observed between the models (only the MATPRO´s upper bias looks qualitatively like Norton's in case of unirradiated material).

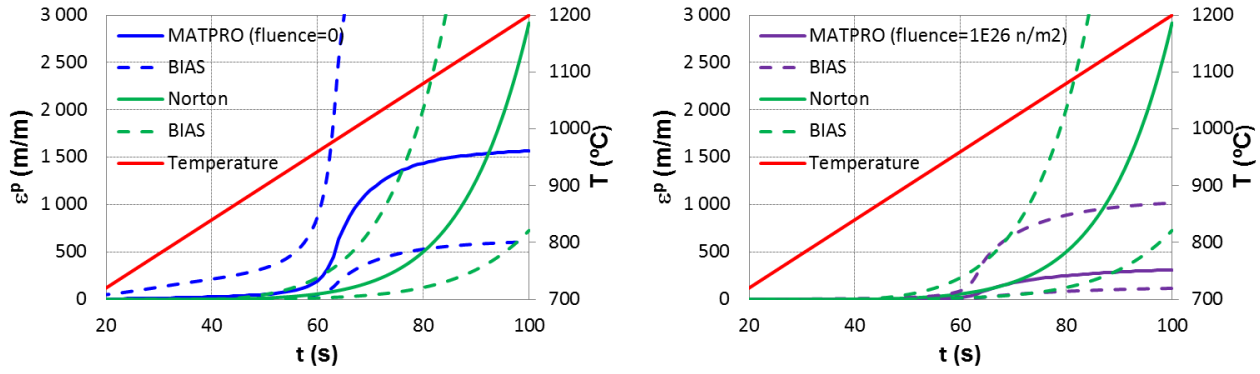

Figure 7. Creep models comparison, bias included, for unirradiated cladding (left) and irradiated cladding (right).

Bias in the failure limits

The bias of the stress and strain limits used by BALON2 for cladding failure in FRAPTRAN has been derived from the scattering of the supporting database, shown in [9]. Figure 7 shows the comparison of the empirical limits with the data. It can be observed an important scattering, being especially relevant in the cladding strain. Based on that, the bias has been implemented in the code through multiplying factors that allow covering the dispersion found (dashed lines in Figure 8). Table 1 shows the values applied for the upper and lower bounds.

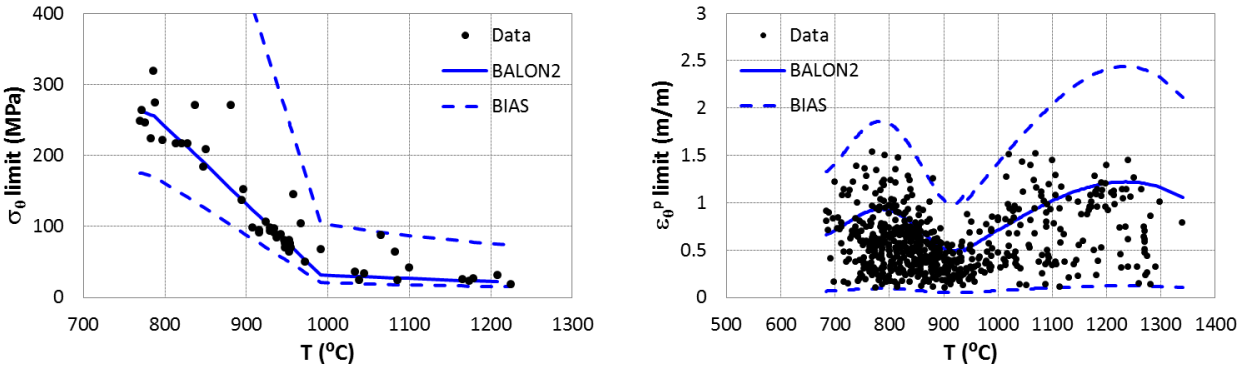

Figure 8. Comparison of the cladding failure limits with data: true hoop stress limit (left) and plastic hoop strain limit (right). Bias included (dashed lines).

Table 1. Factor of limits bias.

Limit	Upper bound	Lower bound
Strain	2	0.1
Stress	3.3	0.7

3.4 Standalone model for axial gas communication (UJV)

Modelling development at UJV focused on the axial gas communication during the LOCA. The standalone model of the gas flow in the fuel rod has been updated with a simplified cladding creep model. In the initial version of the model, the rod was characterized only by the pellet-cladding gap equivalent hydraulic diameters. The current version stores separately fuel outer radius, clad inner radius and clad thickness. A Norton creep law based on the Zry-4 model developed previously for the TRANSURANUS code at TUV Nord has been included in the standalone model [16]. An effective stress in the cladding is calculated with a thin-walled cylinder approximation – considered as sufficient for the testing of the standalone model under realistic boundary conditions. Nevertheless, a more refined approach is needed for the final application and should be achieved by coupling with the TRANSURANUS code. The current version of the standalone module was used to test the explicit-implicit internal coupling of the creep and the gas flow models.

On one hand, the gas flow equations are treated in a fully-implicit iteration loop by a Newton-Raphson method. On the other hand, the creep rate is evaluated explicitly based on rod internal pressure at the end of the time step. The time step length of this explicit step is governed by the maximum allowed strain increment of the cladding.

The results of the test-runs of the standalone model for a WWER-440 rod geometry with simplified LOCA boundary conditions (constant “low” system pressure, constant axial temperature profile peaking at the half of the fuel rod height) are shown below, comparing the pressure evaluated at the plenum of the rod and in the ballooning region. While for the large gap, there is no pressure difference between the plenum and the balloon, a noticeable difference

is observed in the case of almost closed gap corresponding to a high burnup fuel (Figure 9). The effect of the delayed pressure equalization results also in differences in the cladding deformation with time (Figure 10). In addition, however, the difference in the initial gas distribution of the modelled rod has a relevant impact and should be further analyzed.

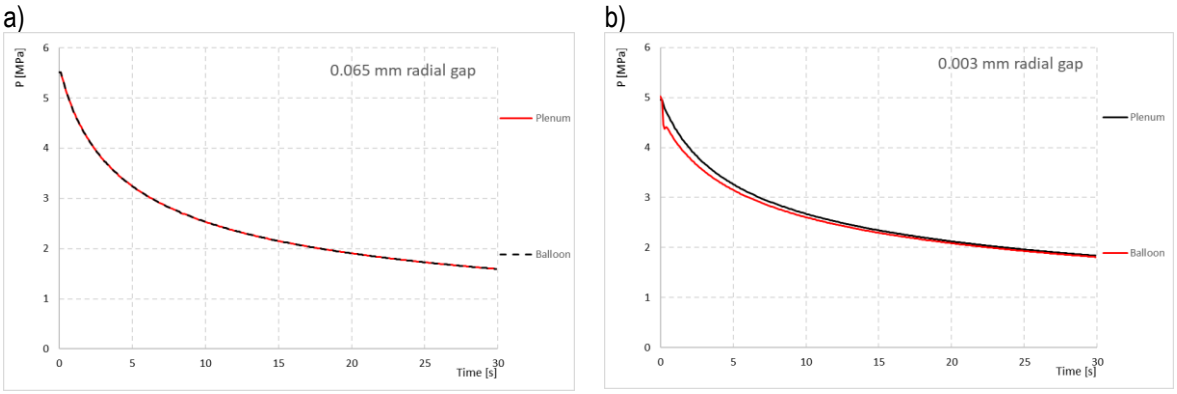

Figure 9: Comparison of inner pin pressure calculated for the plenum and for the axial ballooning zone for (a) large and b) small initial gap sizes as function of time at LOCA.

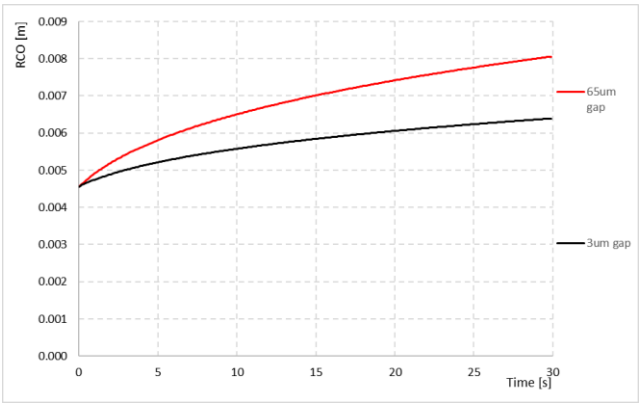

Figure 10: Calculated cladding outer radius as function of time at LOCA for large and small initial gap sizes. See text for details

The current work confirms the feasibility of applying the explicit-implicit approach for calculating both cladding creep and gas flow in the free volume of the fuel rod.

As a next step, the standalone model is being tested with realistic WWER-440 and WWER-1000 boundary conditions transferred from the TRANSURANUS code (loose coupling).
This work was started with the WWER-1000 case as it should be more limiting due to larger gap inventory. In order to facilitate the licensing of alternative suppliers for WWER fuel, the calculations were initiated simulating both TVEL supplied WWER-1000 fuel, as well as the modern Westinghouse WWER-1000 fuel design. The work performed in the project demonstrated first simulations coupling deformation to rod inner gas transport under LOCA conditions. Beyond the R2CA project, such work should be pursued to better understand the gas flow impact on the balloon development.

4. Coupling of simulation tools

4.1 Couplings for TRANSURANUS

The multi-scale modelling approach of the fuel rod behaviour gained interest over the last decades, aiming at improving the fuel performance simulation under various reactor conditions. Within this framework, integral fuel performance codes can be coupled with lower-length mesoscale modules to exploit their physics-based description of the fission gas release and fuel swelling. This results in coupled-code versions that benefit from both the code features and maintain a reduced computational cost. In this work, we present the coupling between the TRANSURANUS fuel performance code and the mesoscale modules MFPR-F and SCIANTIX.

The JRC has been working closely with IRSN and POLIMI on a refined two-way coupling of the TRANSURANUS fuel performance code with the mechanistic chemistry code MFPR-F and the 0D grain-scale code Sciantix, tailored for fission gas behavior modelling. Either of these two mesoscale codes can now be called as point model for each fine zone of the TRANSURANUS nodalization. In addition to a detailed evaluation of the local concentrations of fission products, the local swelling strain is simulated by either MFPR-F or Sciantix and fed back to the total strain calculation by TRANSURANUS. Both Sciantix and MFPR-F are implemented as an optional plug-in to TRANSURANUS (i.e. replacing a dedicated blind interface) that can be provided to the user if licensing conditions are fulfilled with respect to POLIMI and IRSN.

An essential item for the analysis of LOCA experiments is the restart capability for simulating refabricated fuel segments in a research reactor after base irradiation e.g. in a commercial nuclear power plant. This functionality has been demonstrated with both MFPR-F and SCIANTIX coupling modes. Results are outlined below and have been presented at two workshops ”Towards nuclear fuel modelling in the various reactor types across Europe” organized for the TRANSURANUS users (JRC online, 28-30 June 2021 and at ENEA Bologna, 22-23 October 2022 – as embedded event after the 3rd R2CA progress meeting).

4.2 Couplings for FRAPCON and FRAPTRAN

FRAPCON [17] is a computer code programmed in Fortran 90, used to calculate the steady-state response of light-water reactor fuel rods during irradiation. The code calculates temperature, pressure, and deformation of the fuel rod and it is designed to generate initial conditions for transient fuel rod analysis with the parent code FRAPTRAN during reactor transients and hypothetical accidents such as loss-of-coolant accidents, anticipated transients without scram, and reactivity-initiated accidents.

Concerning the fission gas behavior, FRAPCON and FRAPTRAN do not describe fission gas release and gaseous fuel swelling through any mechanistic approach. The models available in the code employ empirical or semi-empirical correlations (e.g., Massih's model, ANS-5.4 or the FRAPFGR model) to calculate the fission gas release, while the coupled phenomenon of the gaseous fuel swelling is treated independently from fission gas release with a model based on Mogensen's data.

A mobility from POLIMI to CIEMAT is underway to include SCIANTIX (an open-source module on inert fission gas behavior developed at Politecnico di Milano) with FRAPCON and FRAPTRAN (proprietary fuel performance codes). The main purposes are to include SCIANTIX as a mechanistic module of fission gas behavior and to improve the predictive capabilities of FRAPCON and FRAPTRAN for representing cladding ballooning in accidental scenarios and accurately estimating gap pressure under transient conditions. As SCIANTIX physical models for fission gas behavior have been improved in R2CA by increasing numerical stability and a priori error control under transient conditions, their inclusion in FRAPCON and FRAPTRAN is expected to improve the overall results.

Coupling verification will be carried out by standard method. Still in the course of the R2CA project, preliminary validation of the FRAPCON/FRAPTRAN/SCIANTIX suite is planned on a selection of irradiation experiments available at both POLIMI and CIEMAT (e.g., experiments from IFA-650 series).

5. Verification and validation

5.1 Testing of TRANSURANUS

JRC has applied the TRANSURANUS code for test simulations of the Halden LOCA experiments IFA-650.10 (Figure 11a-b, Figure 12a-b) and IFA-650.11 (Figure 11c-d, Figure 12c-d). The main technical objectives were:

- confirming the convergence of the newly implemented coupled modes for complex simulations incl. restart modification
- making a first comparison with default options applied in the most recent benchmark, i.e. the IAEA FUMAC CRP
- verifying the consistency with ongoing extensions of TRANSURANUS in parallel Horizon EU projects (e.g. improved material properties and numerical algorithms)

To this end, four different input options for simulating fission product behavior were applied:
FGMech=0: The URGAS model (as TRANSURANUS default)
FGMech=1: The mechanistic fission gas behavior and gaseous swelling model according to G. Pastore [18]
FGMech=3: the 0D grain-scale code Sciantix, called as point model
FGMech=4: the mechanistic chemistry code MFPR-F, called as point model

For this final task report all results were updated with the latest TRANSURANUS version (v1m4j22). The outcome is illustrated for both analysed LOCA cases as follows:
Figure 11a and c: total fission gas release as function of time (incl. base irradiation)
Figure 11b and d: total amount of Xe in the rod free volume as function of time (till the end of the base irradiation)
Figure 12a and c: inner pin pressure as function of time of LOCA
Figure 12b and d: cladding outer radius as function of time of LOCA (at axial location of maximum ballooning)

The abovementioned four different options for simulating fission product behavior lead to considerable differences in both kinetics and level of total fission gas release, already in the base irradiation. This point requires further analysis, as the results of the two approaches previously available in TRANSURANUS are rather close to each other (Figure 11). The different levels of total amount of fission gas must be carefully accounted for later evaluating the eventual release of radioactive fission products (addressed in WP4). Note that the LOCA irradiation experiments and their simulations cannot give information on these total amounts because the fuel segments were refabricated before the LOCA tests. The time axis in Figure 11b and d thus shows the base irradiation only and the y-axis indicates a lower bound for the total amount of Xe in the free volume at end of LOCA.

Nonetheless, for all applied options the simulated increase of fission gas release in the LOCA phase is small and the various approaches for simulating fission product behavior should have only a small impact on cladding deformation and rupture. This assumption is confirmed for both mesoscale approaches in terms of the simulated cladding ballooning and time of burst (with final differences below 2 s, cf. Figure 12a and c). There is also fair agreement with experimental data of the FUMAC project that is supported by uncertainty analyses.

Figure 12b and d show thus only the TRANSURANUS default option of fission product behavior. Both figures include the calculated bounds related to the 5% and 95% percentiles obtained from 200 Monte-Carlo runs applying Gaussian probability distribution functions to a set of 24 input parameters for fuel rod/manufacturing data, boundary conditions, physical properties and key models [19], and illustrate an uncertainty analysis (histogram) of the time and the axial location of burst. The marker ‘experiment’ corresponds to the measured maximum final cladding outer radius while the bar illustrates the axial span of the simulated slice.

The fair agreement is underlined by a comparison with a large set of fuel performance codes in the final FUMAC report [1]. Note that this analysis (Figure 13) includes the Studsvik case (NRC-192) further addressed by IRSN.

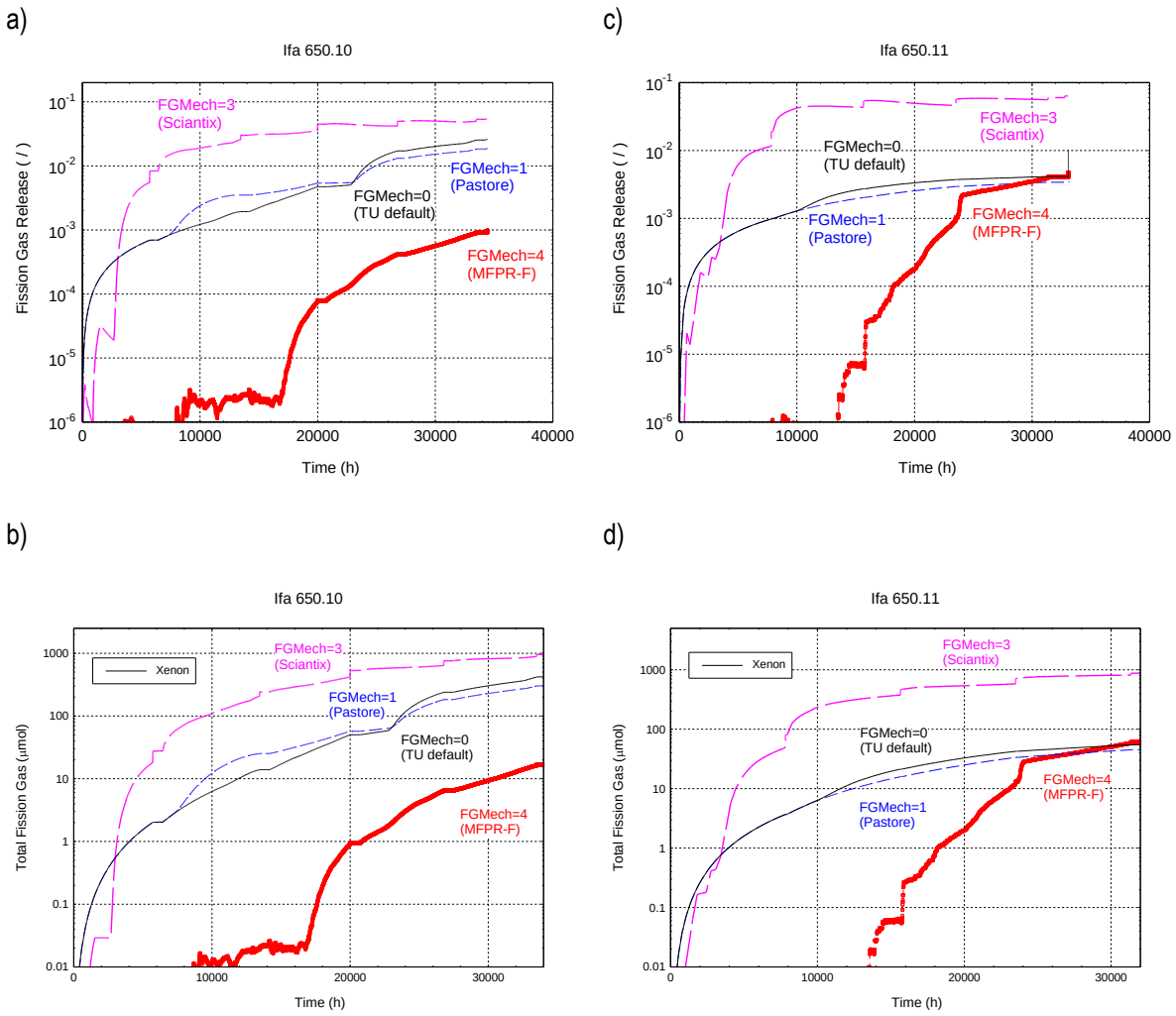

Figure 11: Total fission gas release (a and c) and total amount of Xe in the rod free volume (b and d - till the end of the base irradiation) as function of time simulated with different options of the latest version of TRANSURANUS, for the Halden LOCA tests Ifa 650.10 and Ifa 650.11, respectively. See text for details.

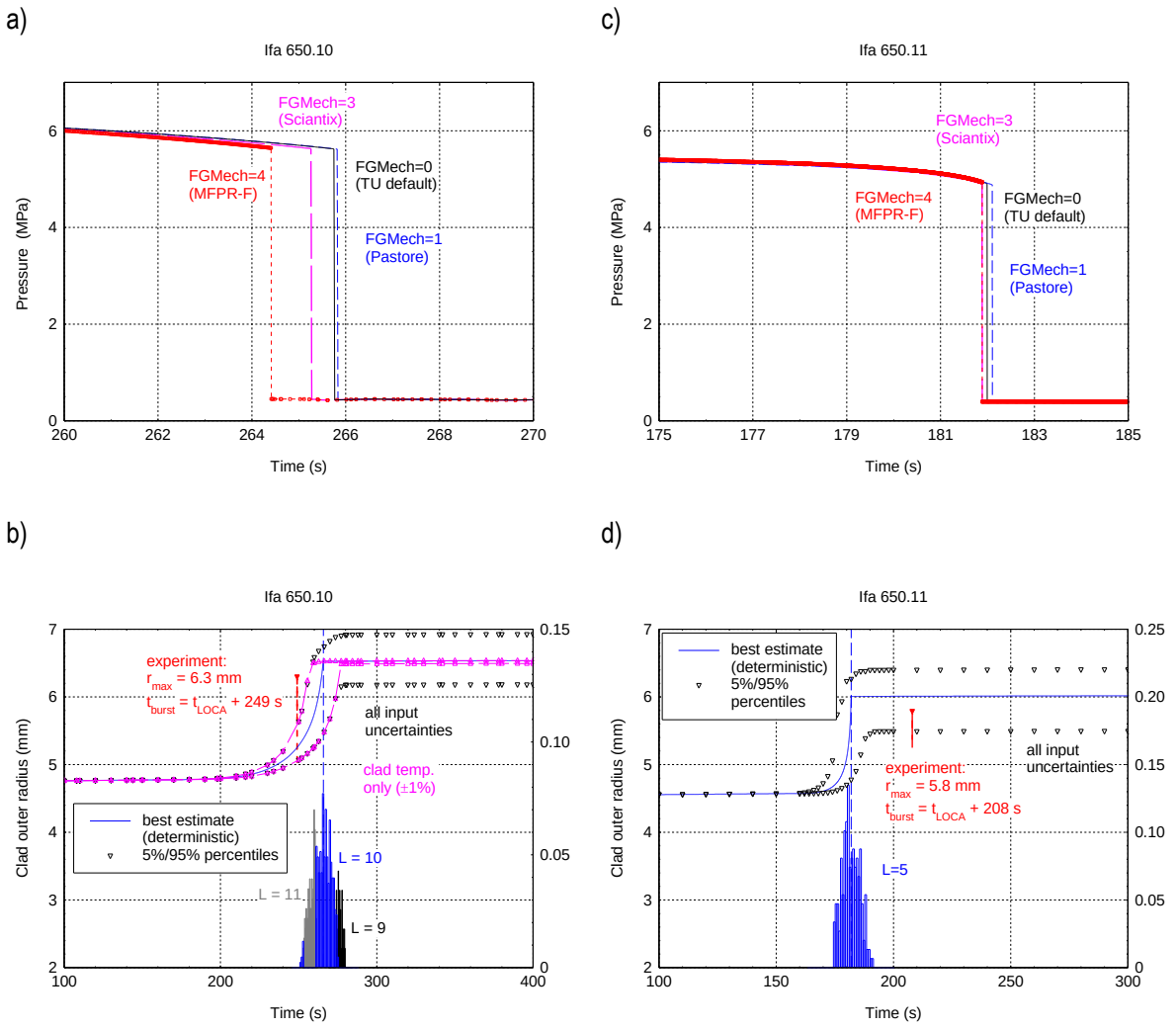

Figure 12: Inner pin pressure (a and c) and cladding outer radius (b and d - at axial location of maximum ballooning) as function of time during LOCA simulated with different options of the latest version of TRANSURANUS, for the Halden LOCA tests Ifa 650.10 and Ifa 650.11, respectively. See text for details.

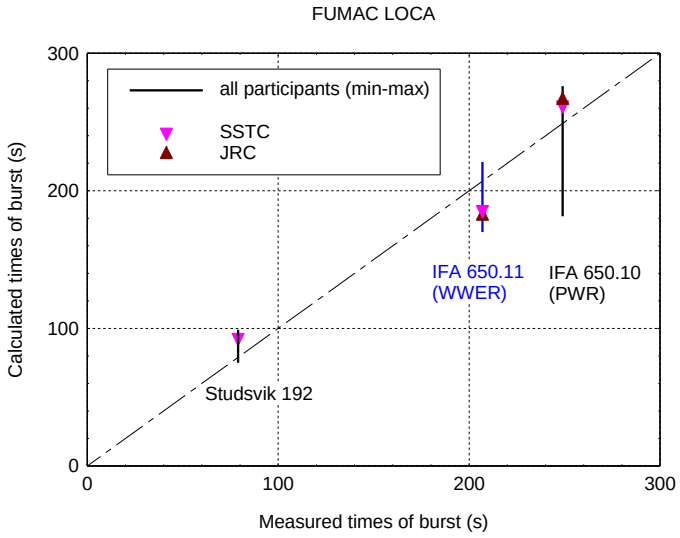

Figure 13: Comparison of measured and calculated times of burst for 3 cases from the IAEA FUMAC project. The markers correspond to TRANSURANUS calculations by users at SSTC and JRC [19] applying independent input decks with a different meshing.

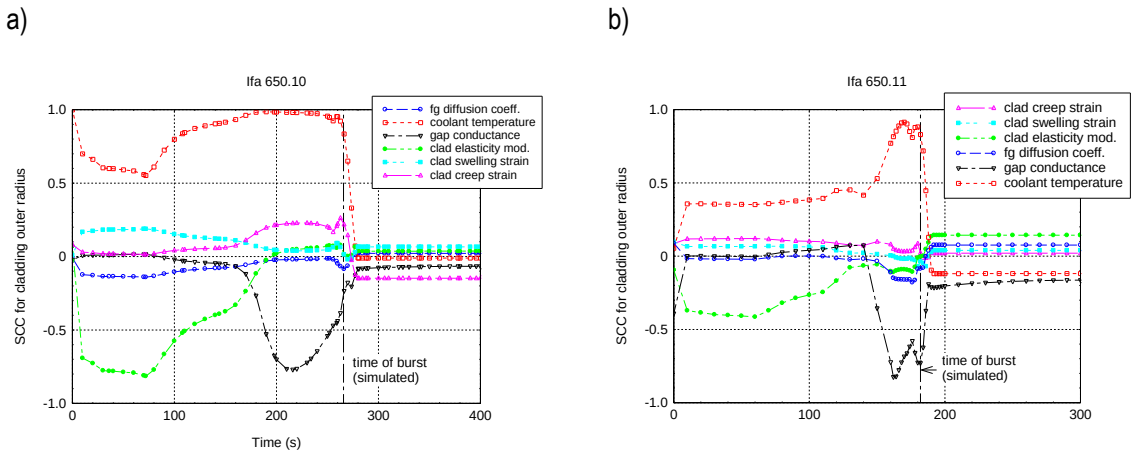

Figure 14: Sensitivity analysis for the cladding outer radius as function of time during LOCA simulated with the latest version of TRANSURANUS, for the Halden LOCA tests Ifa 650.10 (a) and Ifa 650.11(b). See text for details.

Based on the above Monte-Carlo runs, a first sensitivity analysis was made using Pearson's simple correlation coefficients (SCC) between the simulated cladding outer radius and 6 different input quantities. Figure 14 shows the evolution of the SCC´s during the LOCA phase and confirms the expected dominance of the prescribed cladding outer temperature for calculating the deformation of the cladding up to the time of burst. Nevertheless, further analysis is needed for concluding on the most relevant cladding material properties and before setting priorities for further development of fuel simulations in LOCA. As a step beyond the current task, an additional scheme of Monte-Carlo runs should be set up and apply restricted input uncertainties.

5.2 Complementary evaluation of TRANSURANUS//MFPR-F

In the first year of the project, IRSN had applied the TRANSURANUS//MFPR-F coupling to the NRC-192 LOCA test, using the TRANSURANUS dataset prepared by SSTC NRS in the framework of the FUMAC project [1]. Since then, developments in the coupling allowed to use the HBS models of MFPR-F in the coupled mode (see section 3.1). Using this extension the LOCA test NRC-192 was re-analyzed, and the details are provided in a dedicated report of LEI [20]. The coupled TRANSURANUS//MFPR-F code has yet to be improved to handle the shutdown periods in operational scenarios and prescribed linear heat rates during annealing periods.

The FG behaviour in the HBS zone has been further addressed in detail. The figure below represents radial profiles of FG repartition among the intragranular domain, the intergranular (HBS) pores, and the released gas, after the LOCA transient. In the restructured area (blue domain), FG located in HBS pores before LOCA is expected to be released by a process involving overpressurization of the pores. It is thus dependent on the pressure levels reached during the transient, which depend on the equation of state (EoS) applied in the model. Thus, as seen on the figure below, two calculations performed with different EoS, namely Perkus-Yevik (left) and Carnaham-Starling EoS (right), result in different amounts of released gas.

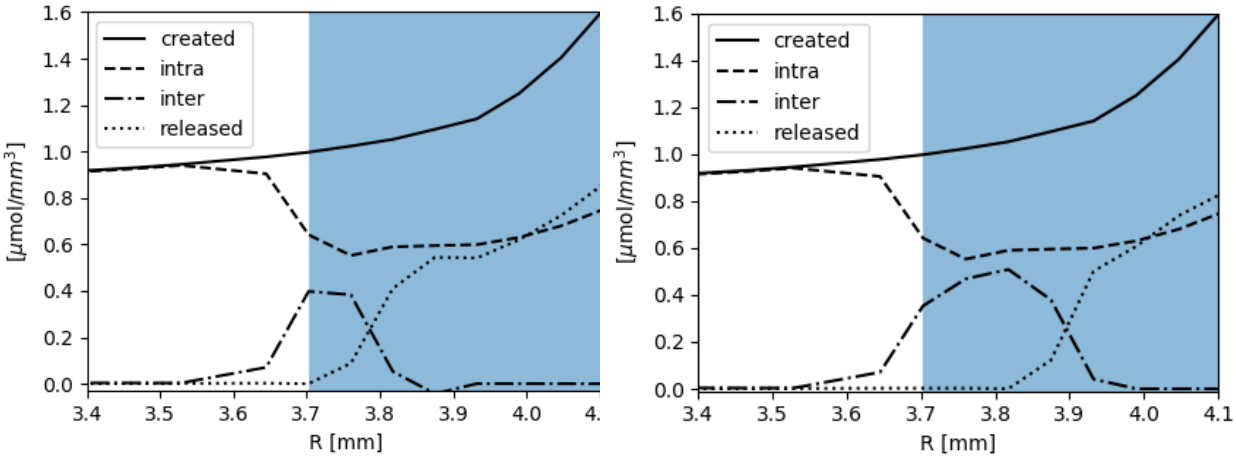

Figure 15: Radial profile of the fission gas created (plain), intragranular (dash), intergranular/HBS pores (dash-dot), and released (dot) after the LOCA transient, obtained with the Perkus-Yevik (left) and Carnaham-Starling (right) equation of states in the HBS pores. The blue stripe corresponds to the extent of the HBS zone.

Apart from equation of state, FG release is found to be sensitive to another parameter of the HBS release model: the pore overpressure criteria ΔP_{crit}. This highlights the need to replace such an empirical parameter by a mechanical criterion for the HBS zone fragmentation, which is expected to be responsible for the FG release [21]. The pellet fractions of FG release obtained with different EoS and/or ΔP_{crit} values are summarized in the table below.

Table 2: Calculated FG release – PY: Perkus-Yevik, CS: Carnaham-Starling

EOS – ΔP_{crit}	FG RELEASE
PY – 300 MPa	4%
PY – 150 Mpa	10%
PY – 100 Mpa	12%
CS – 150 MPa	7 %

5.3 Complementary evaluation of TRANSURANUS//SCIANTIX

The new capability of TRANSURANUS//SCIANTIX has been assessed via the simulation of two experiments from the HATAC programme. This programme comprised the irradiation of two fuel segments extracted from pre-irradiated PWR fuel rods in the SILOE test reactor. The objective of the experiment was to understand which fission gas release mechanisms were involved at high burnup (greater than 35 GWd/t_{HM}) and during power cycling operations. The two sections were cut from fuel rods irradiated in the Fessenheim 1 reactor up to an average burnup of 33.3 MWd/kg_{UO2} and 45.8 MWd/kg_{UO2}. The base irradiation histories were typical of a commercial irradiation operation with a maximum linear heat rate of 22.5 kW/m.

Figure 16 and Figure 17 collect the results of TRANSURANUS//SCIANTIX compared with experimental measurements in terms of stable fission gas release for the base irradiation (only final value) and for the re-irradiation (online measurement). The current model capability tends to overestimate the release occurring during base irradiation, due to an overestimation of the release from grain boundaries predicted in correspondence of power ramps and ascribed to micro-cracking of the grain faces. The overestimation of stable fission gas release is not present during the re-irradiation. Overall, the TRANSURANUS//SCIANTIX results are compatible with the experimental ones (typical acceptability for stable fission gas release is within a factor of two, higher for low release such as during the base irradiation) and improves the standalone TRANSURANUS calculations

Figure 18 to Figure 20 show computed release rate of the short-lived ^{133}Xe against the experimental data measured during the HATAC C2 power transients. The release rate of radioactive gaseous fission products is a new output computed directly in the version of TRANSURANUS coupled with the SCIANTIX module. Calculations exhibit a reasonable behaviour during the power transient. More details on the SCIANTIX mechanistic modelling of radioactive gaseous fission products and results are available in the R2CA public deliverable D4.4 and in a journal publication [8].

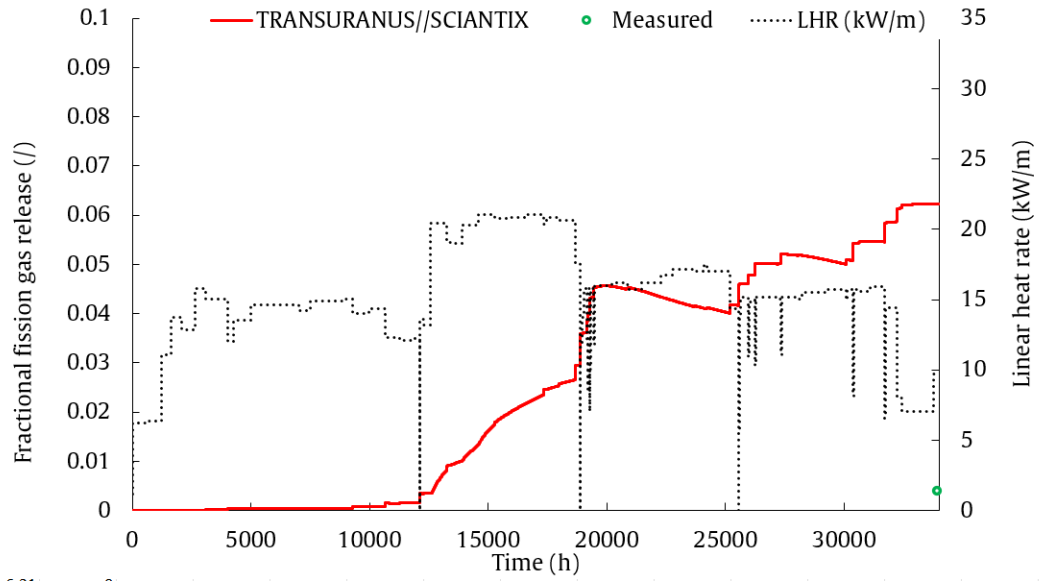

Figure 16: Computed fission gas release during HATAC C2 base irradiation.

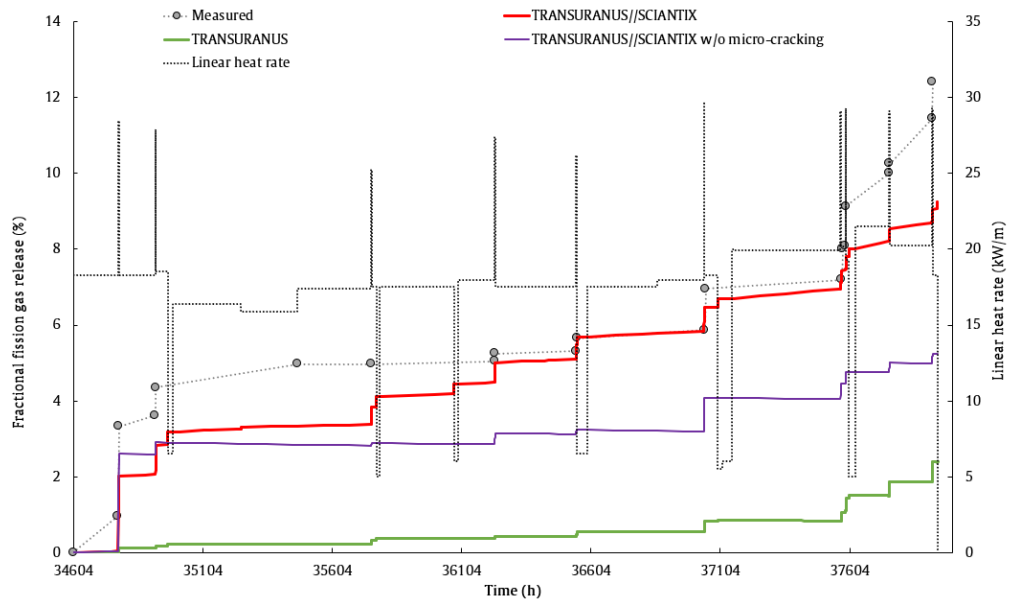

Figure 17: Computed fission gas release during HATAC C2 re-irradiation, against experimental data.

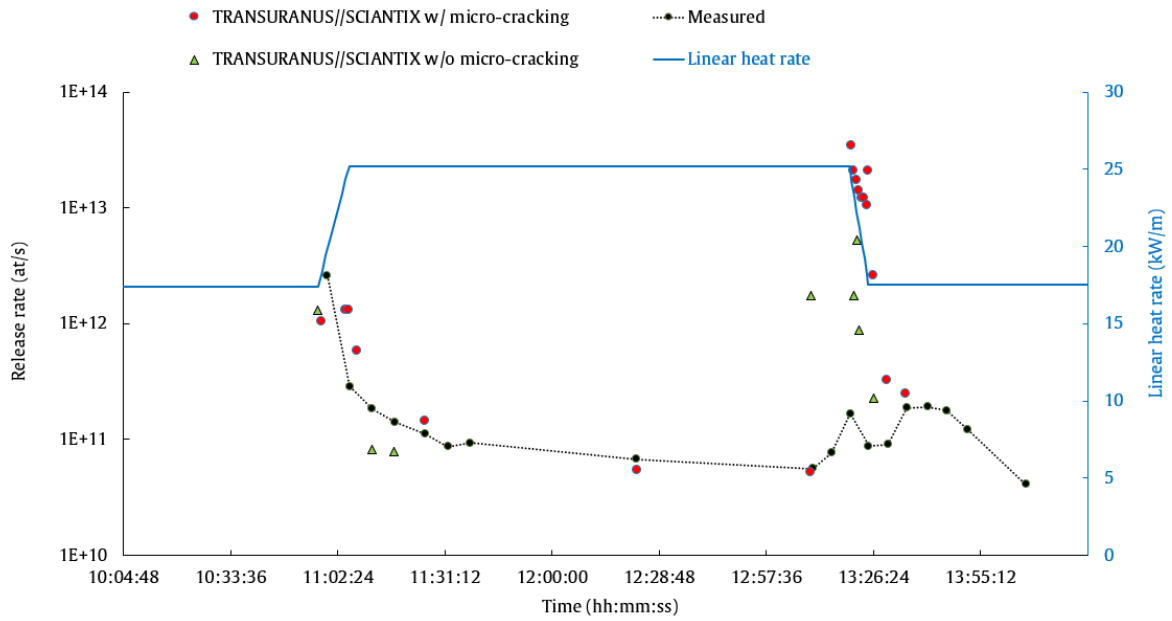

Figure 18: HATAC C2 re-irradiation, focus on 3th transient.

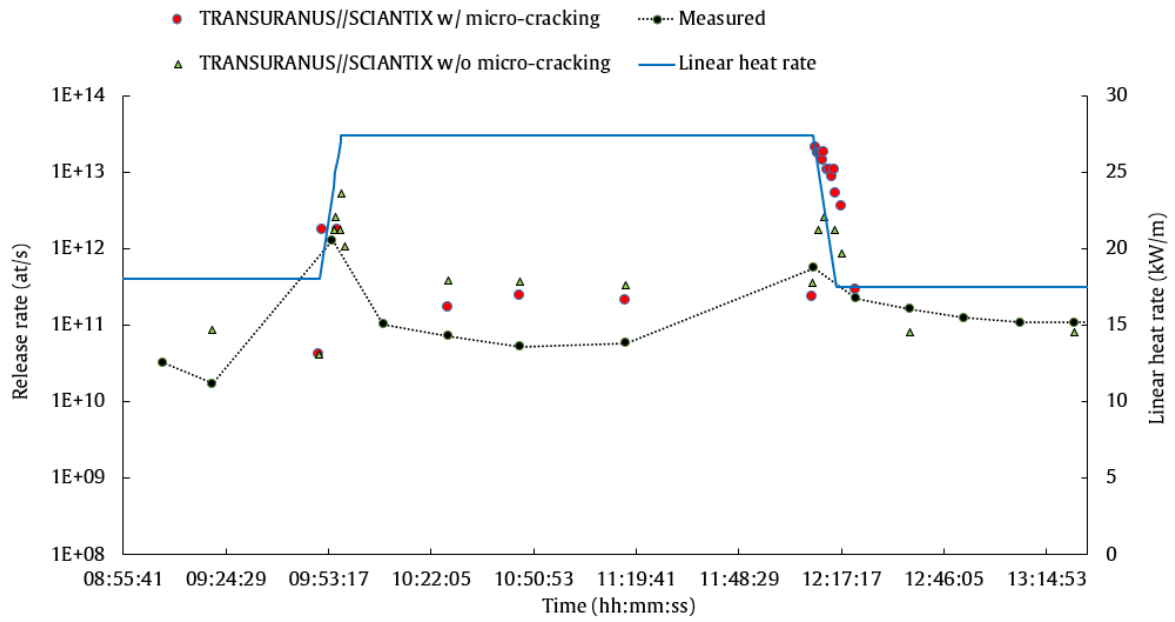

Figure 19: HATAC C2 re-irradiation, focus on 4th transient.

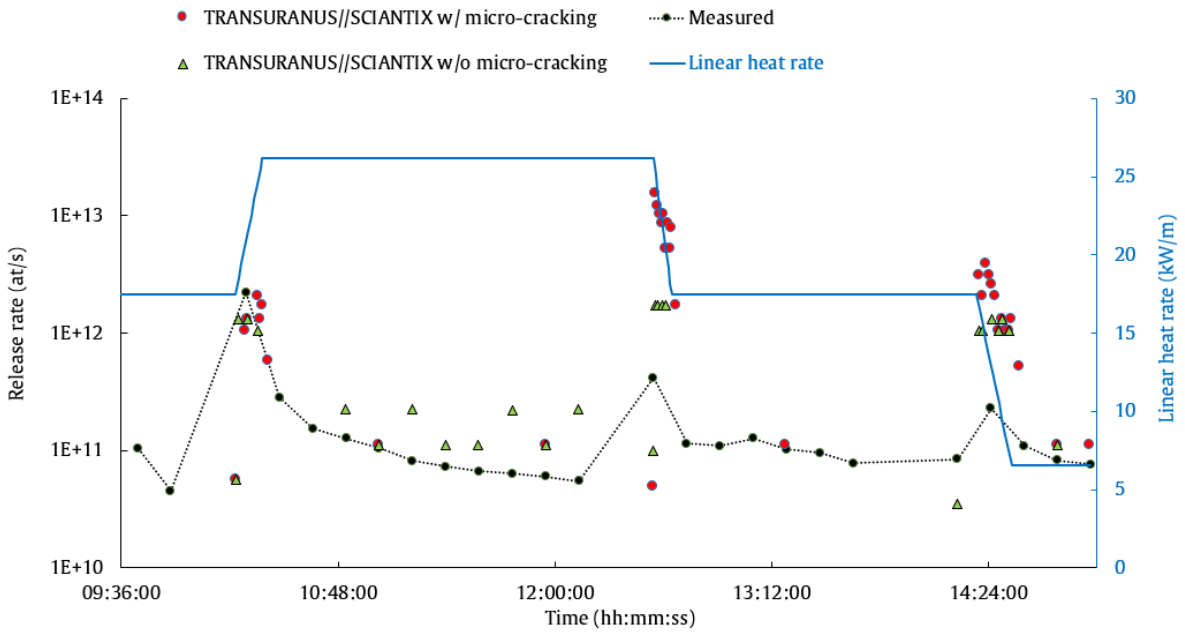

Figure 20: HATAC C2 re-irradiation, focus on 5th transient.

As for the modelling of high burnup structure formation and evolution, the work focused on the model in the SCIANTIX code. The first step of the model concerns the transition from the non-restructured fuel grain structure to the high burnup structure [22]. This irreversible process is modelled via a KJMA approach fitted on experimental data regarding the restructured volume fraction as a function of the local effective burnup [23], i.e., the burnup integrated below 1000°C. The depletion of fission gases from the grains observed during the formation of the high burnup structure is modelled via conventional fission gas diffusion, averaging among restructured and non-restructured grains and accounting for the time-dependent variation of the fraction of restructured fuel volume. To

corroborate the predictive capabilities of this model, we performed an uncertainty analysis propagating to the intra-granular xenon concentration (directly proportional to the solid swelling) the uncertainty associated to each model parameter. Figure 21 reports the results of this analysis depicting the uncertainty bound associated to the retained gas concentration (related to the solid swelling) as a function of the effective burnup. In terms of normalized variance (Figure 22), it is evident that the maximum uncertainty on the retained gas concentration is expected at around 90 GWd/t_{UO2}, i.e., when the formation of the high burnup structure is almost completed. This information is important to assess the uncertainty sources of pellet cladding mechanical interaction, allowing for more accurate (or more conservative) assessment of the cladding conditions prior to a LOCA event.

Lastly, it is also clear that by adopting a more physics-based model, one expects higher uncertainty associated to the output of interest, since these models typically involve more parameters. Therefore, another important point is the informed possibility of using either a semi-empirical or physics-based model depending on the acceptable uncertainties. This activity has been performed in the frame of Master of Science thesis at POLIMI (B. Meleqi).

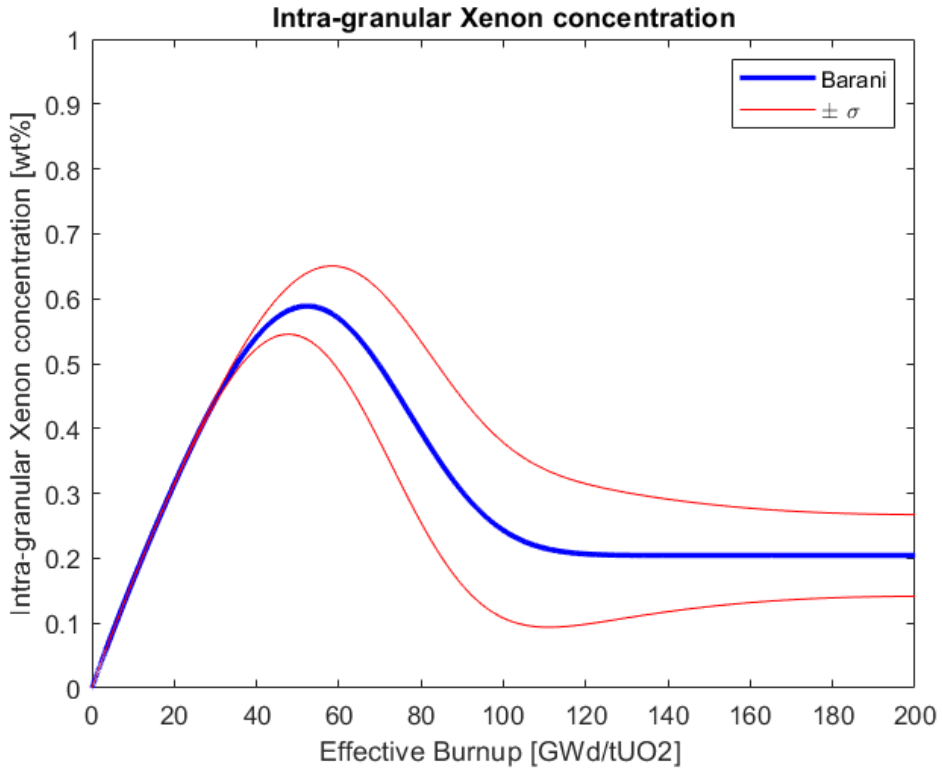

Figure 21: Uncertainty analysis on the intra-granular xenon concentration, obtained by propagating the uncertainty associated to the physical parameters of the model by Barani et al. [22].

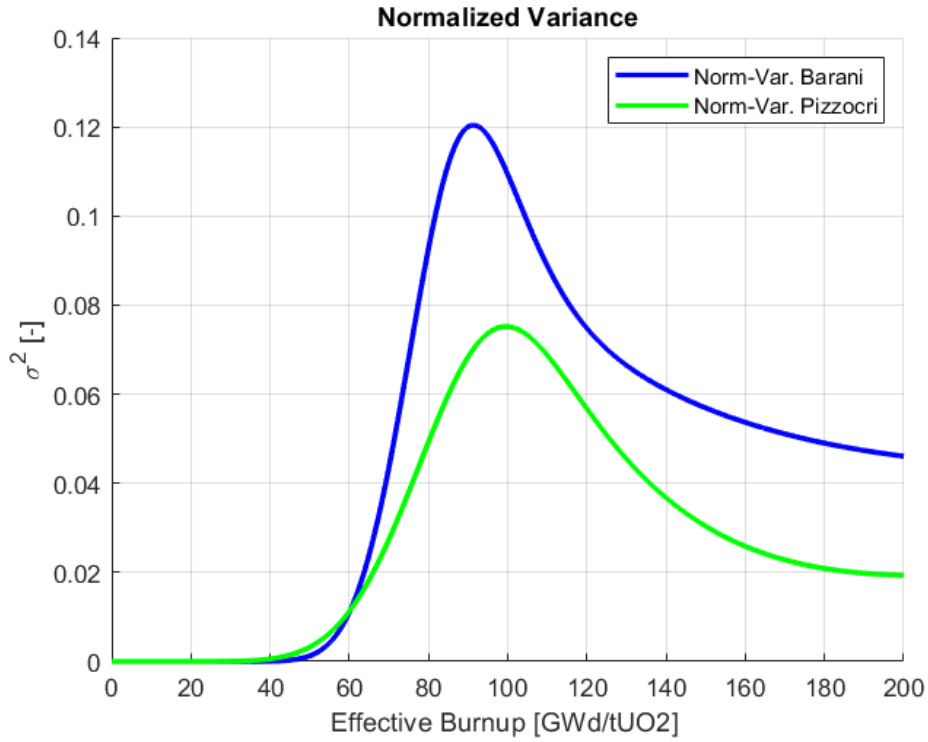

Figure 22: Normalized variance on the intra-granular xenon concentration during the formation of high burnup structure. Results for the physics-based model by Barani et al. [22] are compared with the semi-empirical model by Pizzocri et al. [24]

5.4 Testing of FRAPTRAN

This section describes the assessment of the FRAPTRAN´s mechanical predictability under LOCA conditions. Previous analyses were done under the frame of the FUMAC project [1]. In this work, the simulations tackled have been updated to the last version of the FRAP family codes (i.e., FRAPCON-4.0, in case of simulation with previous irradiation, and FRAPTRAN-2.0), taking into account the new adaptations implemented (shown above) to deepen in the discussions of the deviations found with the modelling by default.

The assessment has been done with two kinds of test: out-of-pile and in-pile. For each test, the following cases have been simulated:

- Best estimate with MATPRO´s correlation for creep (BE).
- Estimation with MATPRO´s correlation for creep plus bias of K, n, m parameters and failure limits (BE+BIAS).
- Best estimate with Norton´s creep law (BE*).
- Estimation with Norton´s creep law plus bias of K, n, m parameters, creep and failure limits (BE*+BIAS).

Additionally, simulations without the bias of the failure limits have been carried out to check their impact (called BE+BIASwoLim. and BE*+BIASwoLim.). Note that in the figures shown in the following sections, in the cases simulated with bias, the bound closer to the experimental data is represented.

5.4.1 Out-of-pile

The tests selected in this case come from the PUZRY series (burst tests) with PWR Zr-4 tubes. Each test entailed a linear operator-defined pressure ramp under isothermal conditions (details shown in [25]). In this work, six PUZRY tests have been simulated with FRAPTRAN by imposing the boundary conditions shown in Table 3.

Table 3. PUZRY tests.

PUZRY	Temperature (ºC)	Pressure rate (bar/s)
26	700	0.119
30	800	0.2663
18	900	0.115
8	1000	0.076
10	1100	0.071
12	1200	0.072

Figure 23 depicts the absolute error obtained in the time-to-failure of each test simulated with the different options implemented in FRAPTRAN. In all the cases, there is a non-negligible underprediction of the best estimate with FRAPTRAN by default (i.e., simulation with MATPRO´s creep model), even if the bias is included. This error is shown to be reduced with the Norton´s creep law, giving rise to overpredictions at temperatures above 900ºC, which can be explained with the corresponding bias (i.e. the resultant uncertainty covers the error). At 900ºC, the error from the underprediction obtained is also covered with the upper bound from the simulation with bias. At temperatures below, it seems that the higher heating rates prevent from being more accurate even with the bias.

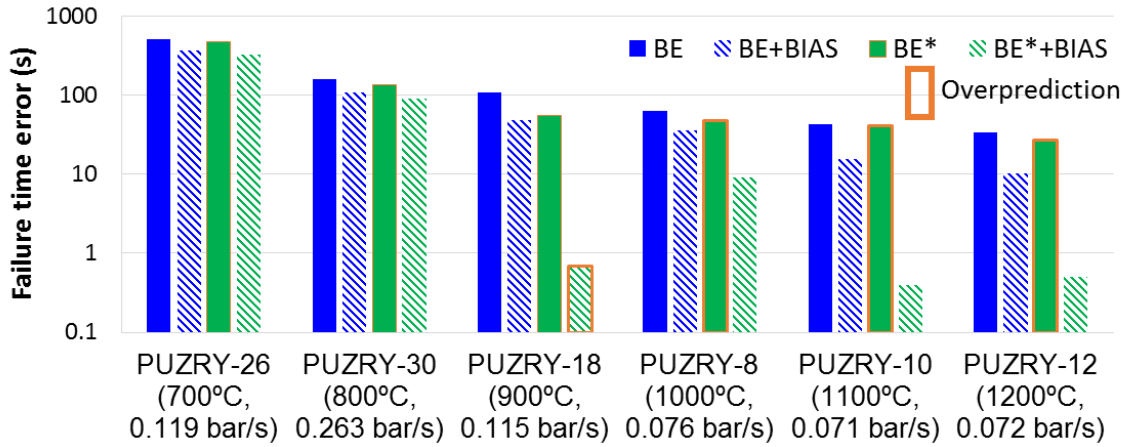

Figure 23. Model-to-data comparison for the time-to-failure of PUZRY tests. Cases with overprediction highlighted in orange.

In order to perform a deeper analysis of the prediction of key variables in the cladding mechanical performance up to the failure, the PUZRY-8 test has been selected. Figure 24 represents the overpressure increase up to burst both measured and predicted. As it can be observed, the bias of K, n and m allows reducing the error obtained with the best estimate of FRAPTRAN by default, although it is not enough to explain the early burst predicted, as previously mentioned. The simulation with the alternative creep modelling (Norton´s law) gives rise to a prediction closer to the data if the corresponding bias is accounted for; indeed, an important impact of the creep model on the time-to-failure predicted is observed. On the contrary, the bias of the failure limits does not show any impact on the prediction. Similar outcomes have been derived from the other tests simulated.

In order to better understand the results obtained with the overpressure increase, an analysis of the cladding strain and stress has been done. First, the FRAPTRAN´s results with the MATPRO´s creep model have been studied (Figure 25). The following observations should be highlighted:

- Failure is due to strain, except when the strain limit is biased, which gives rise to failure due to the stress.
- The sharpen increase of the strain and stress close to the time-to-failure prevents from any effect of the bias of the failure limits.
- The lower strain related to the K, n and m bias allows delaying the ballooning and, as a consequence, the time-to-failure. In fact, the impact of this bias on the small deformations is the main contribution for the resultant delay in the time-to-failure. Minor impact of this bias is observed during ballooning.

Finally, in order to analyse the effect of the creep model on the cladding strain, Figure 26 depicts the results obtained with the best estimate of both the MATPRO´s correlation and the Norton´s law. The Figure shows how the lower deformation of the Norton´s law during ballooning gives rise to a strong impact in the delay of the time-to-failure (stronger than the impact of the bias of K, n and m).

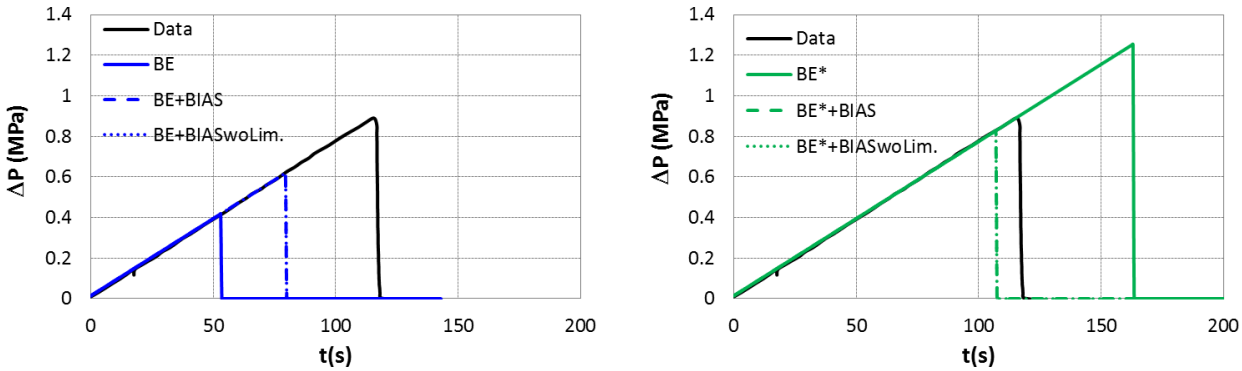

Figure 24. Model-to-data comparison for the overpressure (ΔP) increase in PUZRY-8. Predictions with MATPRO´s creep model on the left and with Norton´s law on the right.

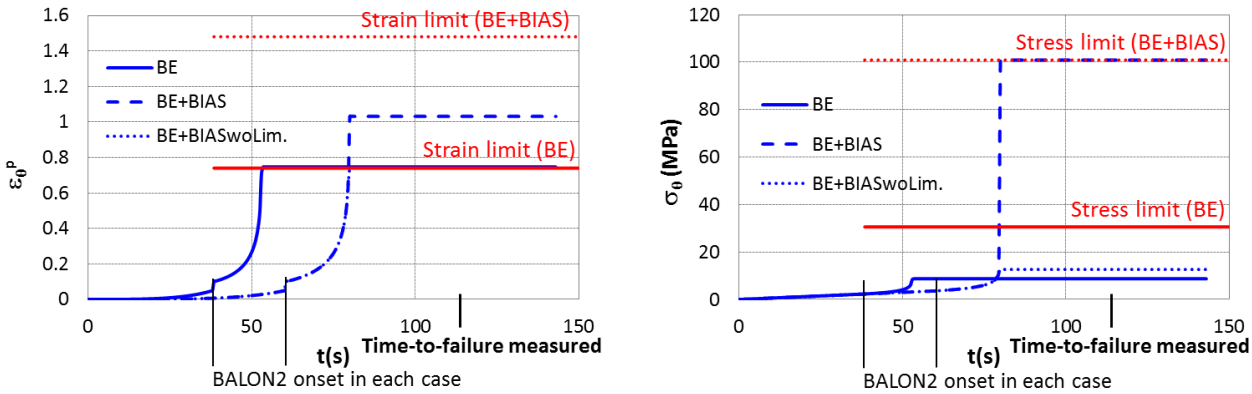

Figure 25. Predictions in PUZRY-8 with MATPRO´s creep model. Cladding plastic hoop strain on the left and hoop stress on the right.

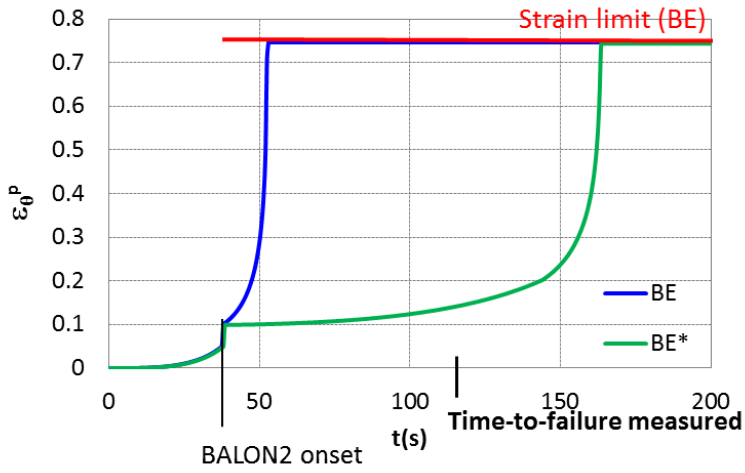

Figure 26. Predictions of cladding plastic strain in PUZRY-8 with MATPRO´s and Norton´s creep models.

5.4.2 In-pile

In order to simulate an irradiated fuel rod under LOCA conditions, the IFA-650.10 test has been selected. It comes from the Halden research reactor that operated under the framework of the OECD-NEA Halden Reactor Project. Particularly, the test simulated belongs to one of its experimental series, IFA-650, that was specifically aimed at testing fuel rodlets under LOCA conditions [26].

The IFA-650.10 test was preceded by a steady state irradiation (61 GWd/tU). Then, the mother rod was refabricated into the test rodlet, which was surrounded by an electrical heater and placed in a high-pressure flask. This device contained instrumentation for measuring rod internal pressure among other relevant variables. A description of the mother rod irradiation, the rodlet tested and the experimental device is given elsewhere [26,27].

The simulation of the LOCA test with FRAPTRAN has been fed with the irradiation conditions of the mother rod, simulated with the steady state fuel performance code FRAPCON, as well as transient thermal conditions specified, both detailed in [28] and [29].

Figure 27 shows the results obtained in terms of the rod internal pressure evolution. The main observations are the following:

- The best estimate simulation with the MATPRO´s creep model (estimation by default) gives rise to early time-to-failure (i.e., underprediction with respect to the measurement), as in the out-of-pile tests.
- An accurate estimation of the upper bound corresponding to the bias of K, n and m parameters is obtained. In other words, this bias may explain the error found with the best estimate. The main contribution to the corresponding uncertainty is related to the small deformation region (before ballooning), as in the out-of-pile tests.
- The bias of the failure limits does not impact to the prediction of the time-to-failure, which is in accordance with the results obtained in the out-of-pile tests.
- The estimation with the Norton´s creep law does not improve the accuracy of the estimation by default, not even with the bias of K, n, m parameters and creep. This should be due to the fact that the Norton´s creep law does not include the irradiation hardening effect, which would delay the time-to-failure (it has been checked that the thermal annealing at the test conditions simulated by the code does not fully recover the irradiation hardening resulting from the base irradiation).

Figure 28 represents the cladding strain and stress evolution for the best estimate with the MATPRO´s creep model. As it can be seen, the failure is due to stress, which sharpen increase at time-to-failure prevents from any effect of the bias of the failure limits. Instead, the lower strain obtained with the bias of K, n and m parameters allows delaying the ballooning and, as a consequence, the time-to-failure (in accordance with the out-of-pile tests results). From Figure 29 it can be deduced that the higher deformation from the Norton´s creep law enlarges the time-to-failure error with respect to the estimation with the MATPRO´s model (irradiation hardening effect included).

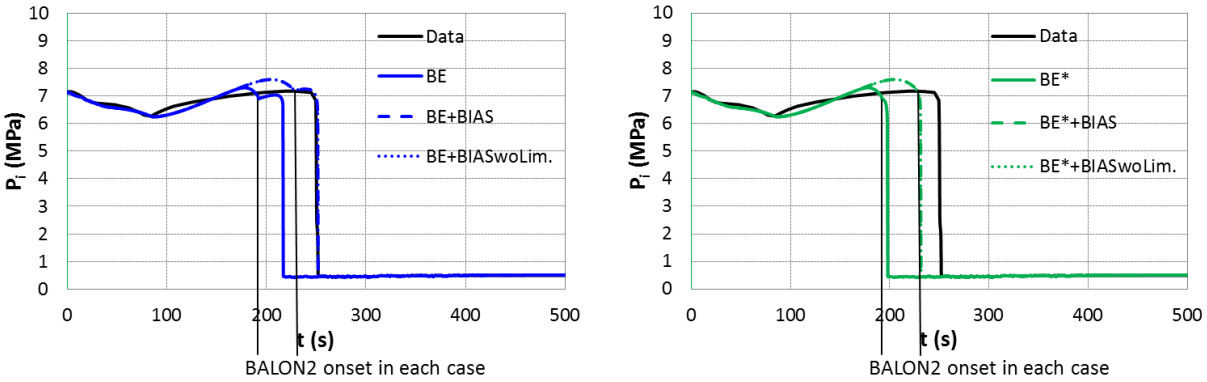

Figure 27. Model-to-data comparison for the internal pressure (P_i) in IFA-650.10. Predictions with MATPRO´s creep model on the left and with Norton´s law on the right.

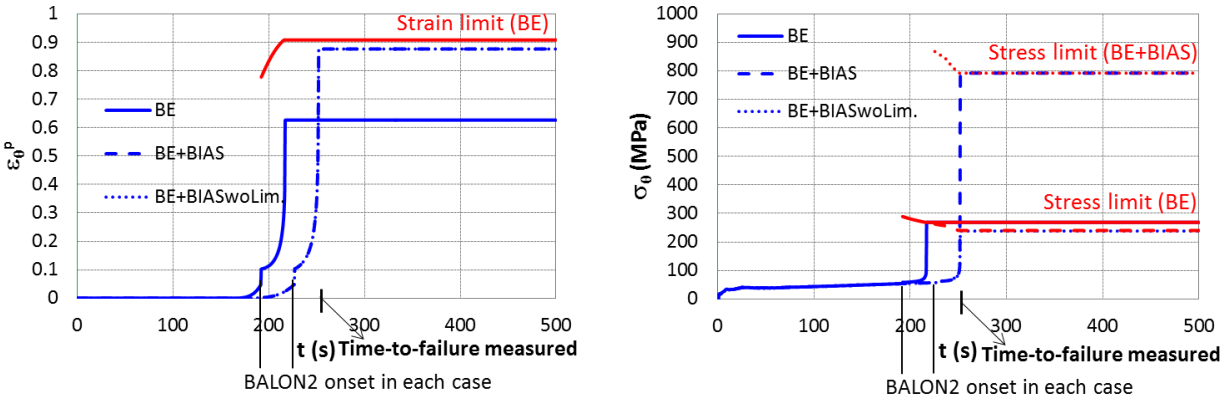

Figure 28. Predictions in IFA-650.10 with MATPRO´s creep model. Cladding plastic hoop strain on the left and hoop stress on the right.

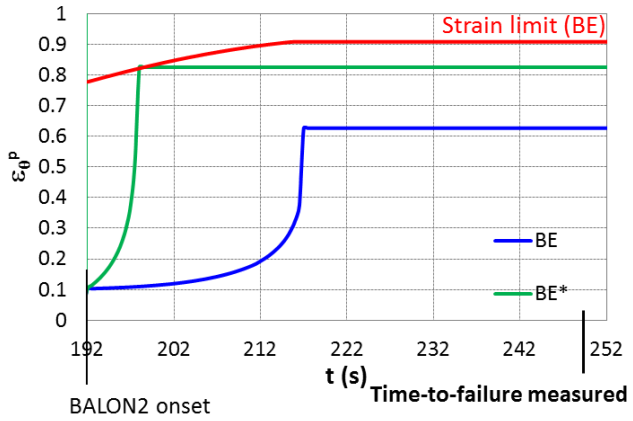

Figure 29. Predictions of cladding plastic strain in IFA-650.10 with MATPRO´s and Norton´s creep models (BE does not reach the strain limit because the failure is due to stress in this case; see Figure 12)

The assessment carried out, based on the simulation of out-of-pile and in-pile tests, allows confirming that FRAPTRAN (applying either MATPRO or Norton creep laws) gives rise to conservative results of the time-to-failure, which is on the safety side. However, depending on the boundary conditions, an important underprediction may be obtained.

Based on the application of the extended code (bias of creep model and failure limits, and alternative creep law), it is concluded that the enhancement of the FRAPTRAN´s accuracy in the time-to-failure prediction goes through properly model the viscoplastic performance of the cladding. In this regard, the Norton´s creep law would be a proper option if the irradiation hardening effect could be accounted for (i.e., data from irradiated cladding would be needed to extend the model). On the contrary, the accuracy enhancement cannot be achieved through the failure limits [10].

6. Service modules for full-core LOCA analysis with TRANSURANUS (SSTC)

In the frame of Task 3.2 (see the dedicated technical report for details), a multistage approach for evaluating fuel rod behaviour during a WWER 1000 Large Break LOCA transient is under preparation. Based on results obtained from RELAP [30] thermal hydraulic models, an update of assembly-wise and pin-by-pin data is prepared.

The updated models are used for preparing input files for fuel performance calculations e.g. by TRANSURANUS. Such LOCA coupled calculations will allow for a realistic evaluation of the mechanical behavior of pellets and cladding.

The general procedure for the calculations performed is as follows. In the first stage, the power of fuel rods was calculated for four cycles using the DYN3D code [31]. The calculation results are stored in separate libraries for all four cycles. In parallel with this, boundary conditions were calculated for modeling the behavior of fuel rods during LOCA. Boundary conditions (external fuel cladding temperature, T_{out}, and external coolant pressure, P_{out}, during LOCA) were calculated using the RELAP5 code in the form of libraries for various fuel-rods power, Kr. Further, using the calculated power of fuel rods and libraries of boundary conditions for T_{out} and P_{out}, the behavior of the fuel rods was simulated using the TRANSURANUS code (v1m3j21). DYN3D and TRANSURANUS calculations were performed for 20 axial layers along the core height. The split is uniform. Libraries of boundary conditions are prepared for 10 layers along the core height. The split is also uniform. When developing the fuel rod model for the TRANSURANUS code, the results of the FUMAC project were used to the maximum, including modeling the behavior of the WWER fuel rod in the LOCA (experiment IFA-650.11, [1],[32]).
Also, within the framework of the project, libraries of accumulation of gaseous fission products during burnup for various types of fuel rods were calculated. The calculations were performed using the SCALE, depletion sequences T6-DEPL software package [33]. Based on these libraries and the characteristics of the release of gaseous fission products from the fuel pellet under the cladding, the release of activity into the primary circuit from failed fuel rods was estimated. The general calculation scheme is shown in Figure 30.

As part of the R2CA project, a dedicated service module was developed for preparing input files of the TRANSURANUS code, running the code, selecting the necessary reference calculation results, and saving files to libraries. The main features of this module are as follows:

- creation of an input file for various types of fuel rods;
- creation of fuel rods' load history before the LOCA. All cycles of operation of the fuel assemblies are taken into account, its movement in the core during refueling, power reduction schedules during shutdowns, and power increase at the startup of the cycle;

- creation of fuel rod power history and boundary conditions during LOCA based on the libraries of T/H boundary conditions and fuel rods power at the beginning of LOCA;
- adjustment (if necessary) of the fuel rod power Kr in the form of $K_r \times K_{eng}$ separately for each fuel cycle;
- execution of the calculation for the full core, symmetry sector and individual assemblies;
- reading from the output files of the necessary reference calculation results;
- determination of the number of failed fuel rods during the LOCA;
- assessment of the activity release to the primary circuit from failed fuel rods;
- saving all input and output files for the possibility of performing additional calculations of individual fuel rods.

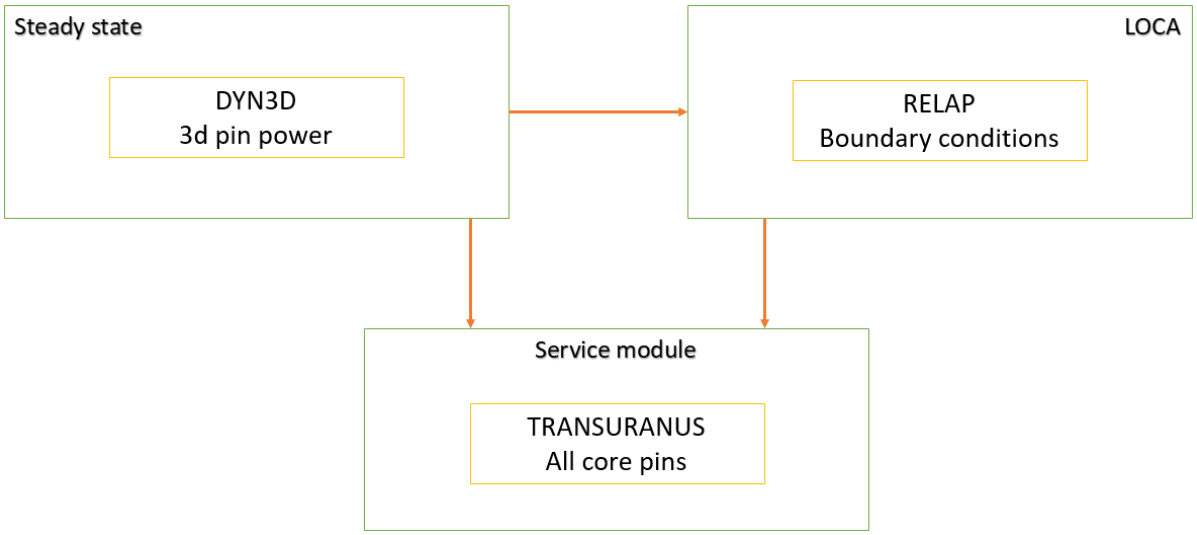

Figure 30 – The general calculation scheme

7. Summary and outlook

As the main achievement of this task in the R2CA project 'Fuel rod behaviour during LOCA', a higher degree of mechanistic modelling has been successfully implemented in the fuel performance codes, along with an improved viscoplastic model of the cladding.

The integral fuel performance code FRAPTRAN has been extended in terms of mechanical modelling, more precisely by adapting an alternative Norton-type creep law and cladding failure limits – including bias options. The FRAPCON code has been coupled with the SCIANTIX mesoscale model. Its evaluation is still underway in the frame of a mobility plan and will be reported separately.

The TRANSURANUS code has been coupled with two mesoscale fuel behaviour codes (MFPR-F and SCIANTIX). Considerable effort has been made to develop plug-in modules that allow for a) feedback from these codes to the integral fuel simulation, including mechanical phenomena as e.g. fuel deformation, and b) applying a re-start modification option as needed for the simulation of a LOCA following a base irradiation in a commercial NPP.

A prototype standalone module for simulating axial gas communication during LOCA has been developed and is being tested with realistic boundary conditions transferred from the TRANSURANUS code (loose coupling). The work was started with the WWER-1000 case - for fuel supplied either by TVEL (Russia) or Westinghouse (Sweden) – but due to priority constraints at UJV (licensing of a fuel supplier alternative to Russia), a full coupling couldn't be achieved within the timeframe of the current task.

In the course of a multistage approach for evaluating fuel rod behaviour during a WWER 1000 Large Break LOCA transient, a service module for off-line interfaces to be used by the TRANSURANUS code has been developed. It makes use of the reactor dynamics code DYN3D and the thermo-hydraulic code RELAP, for pre-calculating the steady state pin power and the LOCA boundary conditions, respectively. The multistage approach for a full-core analysis allows for assessing the number of failed rods and hence the radioactive fission product release to the primary coolant in the event of LOCA.

For the assessment of the modified simulation tools, a number of cases from the global database has been selected consisting of two LOCA experiments of the Halden Reactor test series IFA 650, one LOCA simulation test performed by Studsvik Nuclear AB, Sweden (NRC-192), as well as 3 transient irradiation experiments at the French Siloe reactor (HATAC C1 and C2, Contact 1). The available experimental data, power histories and boundary conditions were used for verification and validation of the coupled code versions. The LOCA cases show a fair agreement with the outcome of the IAEA FUMAC project, and a small impact of the various approaches for simulating fission product behaviour on cladding deformation and rupture.

First uncertainty and sensitivity analyses for the LOCA phase of IFA 650.10 and IFA 650.11 confirm the expected dominance of the cladding outer temperatures for calculating the deformation of the cladding up to the time of burst, and indicate the importance of cladding material properties, as creep, swelling and the elasticity module.

The code coupling TRANSURANUS//SCIANTIX has been further tested with the case HATAC C2. An uncertainty analysis using the normalized variance of the retained intra-granular Xenon concentration revealed that its maximum uncertainty is expected immediately before completing the formation of the HBS.

The code coupling TRANSURANUS//MFPR-F was used for further analysis of the case NRC-192, since the coupling now contains the HBS models of MFPR-F. The prediction of fuel restructuring based on the evolution of the dislocation density was found to be satisfactory, although at present it requires to disregard the shutdown periods from the power history. Regarding the LOCA transient, FG release from the HBS zone was calculated using a model based on the pressure in a HBS pore. Although its predictions are satisfactory, the model is empirical and can be improved by means of a more mechanistic approach.

Finally, the extended FRAPTRAN code has been verified using the IFA 650.10 LOCA test and the standalone PUZRY tests (both taken from the IAEA FUMAC project). Improvements in the time-to-failure prediction are primarily linked to the viscoplastic performance of the cladding while modified failure limits will not lead to higher accuracy. A final implementation of Norton´s creep law would require the irradiation hardening effect to be included.

8. References

[1] "Fuel modelling in accident conditions (FUMAC), Final report of a coordinated research project", IAEA CRP T12028 (2014-2018), IAEA-TECDOC-1889, IAEA, Vienna, Austria, 2018.

[2] "International Fuel Performance Experiments (IFPE) Database", OECD-NEA Nuclear science Working Party on Scientific Issues of Reactor Systems, 2018, http://www.nea.fr/html/science/fuel/ifpelst.html.

[3] M. Charles, C. Lemaignan, Fuel performance under normal PWR conditions: A review of relevant experimental results and models, Journal of Nuclear Materials 188 (1992) 96.

[4] M. S. Veshchunov, V. D. Ozrin, V. E. Shestak, V. I. Tarasov, R. Dubourg, G. Nicaise, Development of the mechanistic code MFPR for modelling fission-product release from irradiated UO_2 fuel, Nuclear Engineering and Design 236 (2006) 179.

[5] F. Kremer, R. Dubourg, F. Cappia, V. V. Rondinella, A. Schubert , P. Van Uffelen, T. Wiss, High Burn Up Structure formation and growth and fission product release modelling: new simulations in the mechanistic code MFPR-F, in: TopFuel2018 (Prague, Czech Republic, 2018).

[6] D. Pizzocri, T. Barani, L. Luzzi, SCIANTIX: A new open source multi-scale code for fission gas behaviour modelling designed for nuclear fuel performance codes. Journal of Nuclear Materials. , Journal of Nuclear Materials 532 (2020) 152042.

[7] G. Zullo, D. Pizzocri, A. Magni, P. Van Uffelen, A. Schubert , L. Luzzi, Towards grain-scale modelling of the release of radioactive fission gas from oxide fuel. Part I: SCIANTIX., Nuclear Engineering and Technology 54 (2022) 2771.

[8] G. Zullo, D. Pizzocri, A. Magni, P. Van Uffelen, A. Schubert , L. Luzzi, Towards grain-scale modelling of the release of radioactive fission gas from oxide fuel. Part II: Coupling SCIANTIX with TRANSURANUS. , Nuclear Engineering and Technology (2022).

[9] K. J. Geelhood, W. G. Luscher, J. M. Cuta, I. A. Porter, "FRAPTRAN--2.0: A Computer Code for the Transient Analysis of Oxide Fuel Rods", PNNL-19400, Vol.1 Rev2, Pacific Northwest National Laboratory, 2016.

[10] "SCDAP/RELAP5/MOD3.3 Code Manual MATPRO - a library of material properties for light-water-reactor accident analysis", NUREG/CR-6150, Rev. 2, INEL-96/0422 USNRC, 2000.

[11] K. J. Geelhood, W. G. Luscher, C. E. Beyer, "Stress/Strain Correlation for Zircaloy", PNNL-17700, Pacific Northwest National Laboratory, 2008.

[12] D. L. Hagrman, "Zircaloy cladding shape at failure (BALON2)", EGG-CDAP-5379, 1981.

[13] V. Di Marcello, A. Schubert, J. van de Laar, P. Van Uffelen, The TRANSURANUS mechanical model for large strain analysis, Nuclear Engineering and Design 276 (2014) 19.

[14] G. Pastore, R. L. Williamson, R. J. Gardner, S. R. Novascone, J. B. Tompkins, K. A. Gamble, J. D. Hales, Analysis of fuel rod behavior during loss-of-coolant accidents using the BISON code: Cladding modeling developments and simulation of separate-effects experiments, Journal of Nuclear Materials 543 (2021) 152535.

[15] H. Rosinger, P. C. Bera, Steady-state creep of Zircaloy-4 fuel cladding from 940 to 1873 K, Journal of Nuclear Materials 82 (1979) 286.

[16] F. J. Erbacher, H. J. Neitzel, H. Rosinger, H. Schmidt, K. Wiehr, "Burst criterion of Zircaloy fuel claddings in a loss-of-coolant accident", ASTM (Ed.), Proceedings of Zirconium in the nuclear industry, Fifth Conference, ASTM STP 754, 1982, p. 271.

[17] K. J. Geelhood, W. G. Luscher, P. A. Raynaud, I. E. Porter, "FRAPCON-4.0: A Computer Code for the Calculation of Steady-State, Thermal-Mechanical Behavior of Oxide Fuel Rods for High Burnup", PNNL-19400, Vol.1 Rev2, Pacific Northwest National Laboratory, 2015.

[18] G. Pastore, L. Luzzi, V. Di Marcello, P. Van Uffelen, Physics-based modelling of fission gas swelling and release in UO_2 applied to integral fuel rod analysis, Nuclear Engineering and Design 256 (2013) 75.

[19] A. Schubert, Z. Soti, P. Van Uffelen, M. Ieremenko, R. Calabrese, S. Boneva, N. Mihaylov, M. Mitev, "The benefit of international benchmarks for extension and validation of the TRANSURANUS fuel perfromance code", Proceedings of Conference on Reactor Fuel Performance - TopFuel 2019, ANS, Seattle, WA, USA, 22-26 September 2019.

[20] A. Tidikas, "TRANSURANUS/MFPR-F coupling investigation (technical report under preparation)", IRSN Cadarache (France), LEI Kaunas (Lithuania), 2022.
[21] J. Noirot, Y. Pontillon, S. Yagnik, J. A. Turnbull, T. Tverberg, Fission gas release behaviour of a 103 GWd/tHM fuel disc during a 1200°C annealing test, Journal of Nuclear Materials 446 (2014) 163.
[22] T. Barani, D. Pizzocri, F. Cappia, L. Luzzi, G. Pastore, P. Van Uffelen, Modeling high burnup structure in oxide fuels for application to fuel performance codes. part I: High burnup structure formation, Journal of Nuclear Materials 539 (2020) 152296.
[23] T. J. Gerczak, C. M. Parish, P. D. Edmondson, C. A. Baldwin, K. A. Terrani, Restructuring in high burnup UO_2 studied using modern electron microscopy, Journal of Nuclear Materials 509 (2018) 245.
[24] D. Pizzocri, F. Cappia, L. Luzzi, G. Pastore, V. V. Rondinella, P. Van Uffelen, A semi-empirical model for the formation and depletion of the high burnup structure in UO_2, Journal of Nuclear Materials 487 (2017) 23.
[25] E. Perez-Feró, C. Győri, L. Matus, L. Vasáros, Z. Hózer, P. Windberg, L. Maróti, M. Horváth, I. Nagy, A. Pintér-Csordás, T. Novotny, Experimental database of E110 claddings exposed to accident conditions, Journal of Nuclear Materials 397 (2010) 48.
[26] A. Lavoil, "LOCA testing at Halden, the tenth experiment IFA-650.10", OECD Halden Reactor Project, 2010.
[27] N. Nishi, B. H. Lee, "Summary of pre-irradiation data on fuel segments supplied by EDF/FRAMATOME and tested in IFA-610, 629 and 648", OECD Halden Reactor Project, 2001.
[28] I. Vallejo, L. E. Herranz, HALDEN LOCA tests: Simulations of IFA-650.3, .5 and .10 with FRAP Serie Codes. Preliminary Results and Comparisons to Experimental Data, in: Enlarged Halden Programme Group Meeting (OECD Halden Reactor Project, Rorøs, Norway, 2014).
[29] L. E. Herranz, S. B. Pelaez, Assessment of FRAPTRAN-1.5 Capabilities for Clad-to-Coolant Heat Transfer under Loss of Coolant Accidents, in: Enlarged Halden Programme Group Meeting (OECD Halden Reactor Project, Fornebu, Norway, 2016).
[30] "RELAP/MOD Code manual, Volume 1: Code structure, system models and solution methods", NUREG/CR-5535, 1995.
[31] U. Grundmann, U. Rohde, S. Mittag, S. Kliem, "DYN3D version 3.2 - Code for calculation of transients in Light Water Reactors (LWR) with hexagonal or quadratic fuel elements - description of models and methods.", FZR-434, Forschungszentrum Rossendorf, 2005.
[32] M. Ieremenko, I. Ovdiienko, "Qualification of TRANSURANUS models for mixed core fuel based on the FUMAC outcome", Proceedings of IAEA Technical Meeting on "Modelling of Fuel Behaviour in Design-Basis Accidents and Design Extension Conditions", Vol. IAEA-TECDOC-1913, 2019, p. 50.
[33] M. A. Jessee, D. Wiarda, K. T. Clarno, U. Mertyurek, K. Bekar, "TRITON: A Multipurpose transport, depletion, sensitiviy and uncertainty analysis module. SCALE code system.", ORNL/TM-2005/39. Version 6.2.3., 2005.